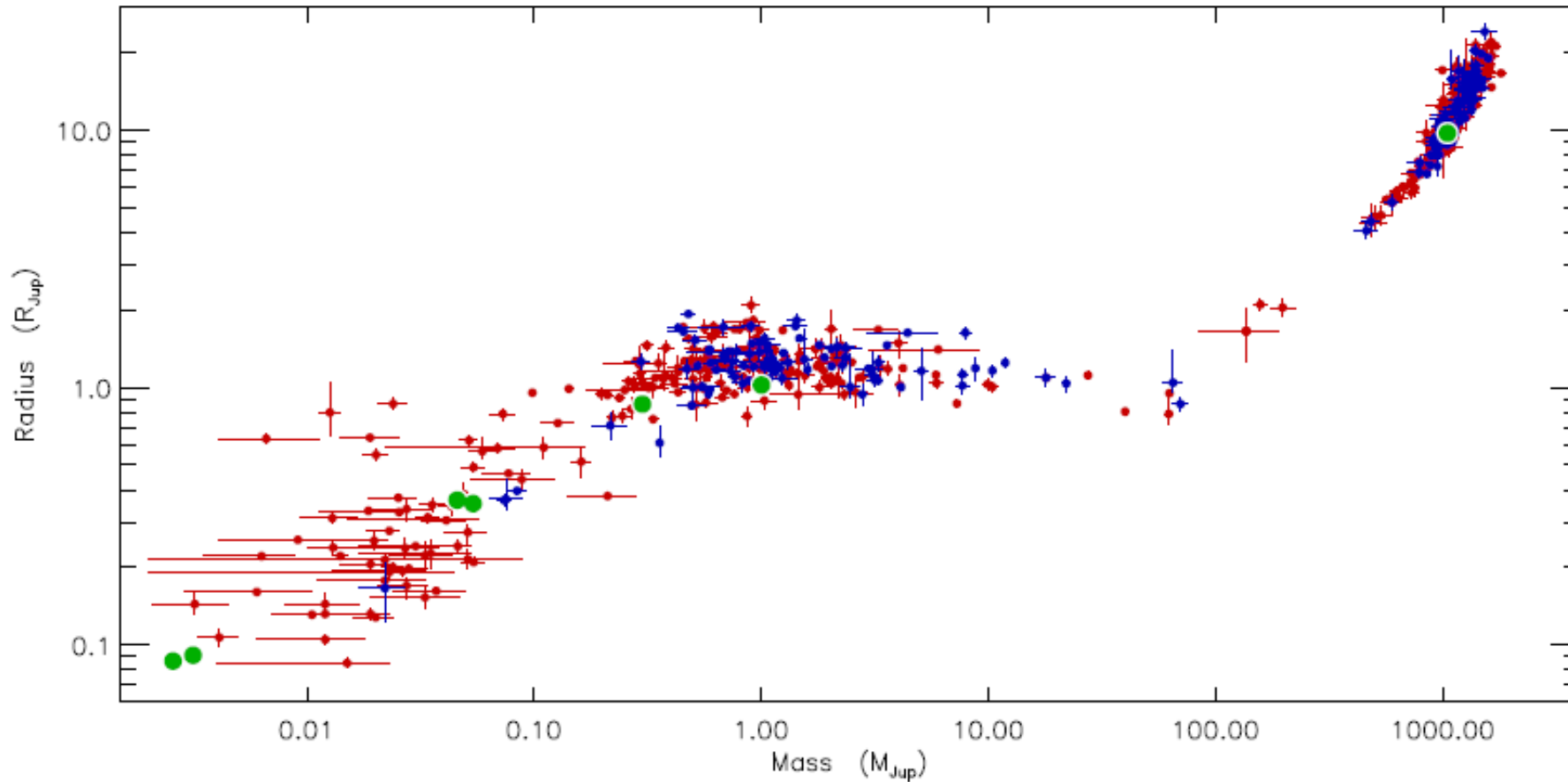


# Planet detection methods

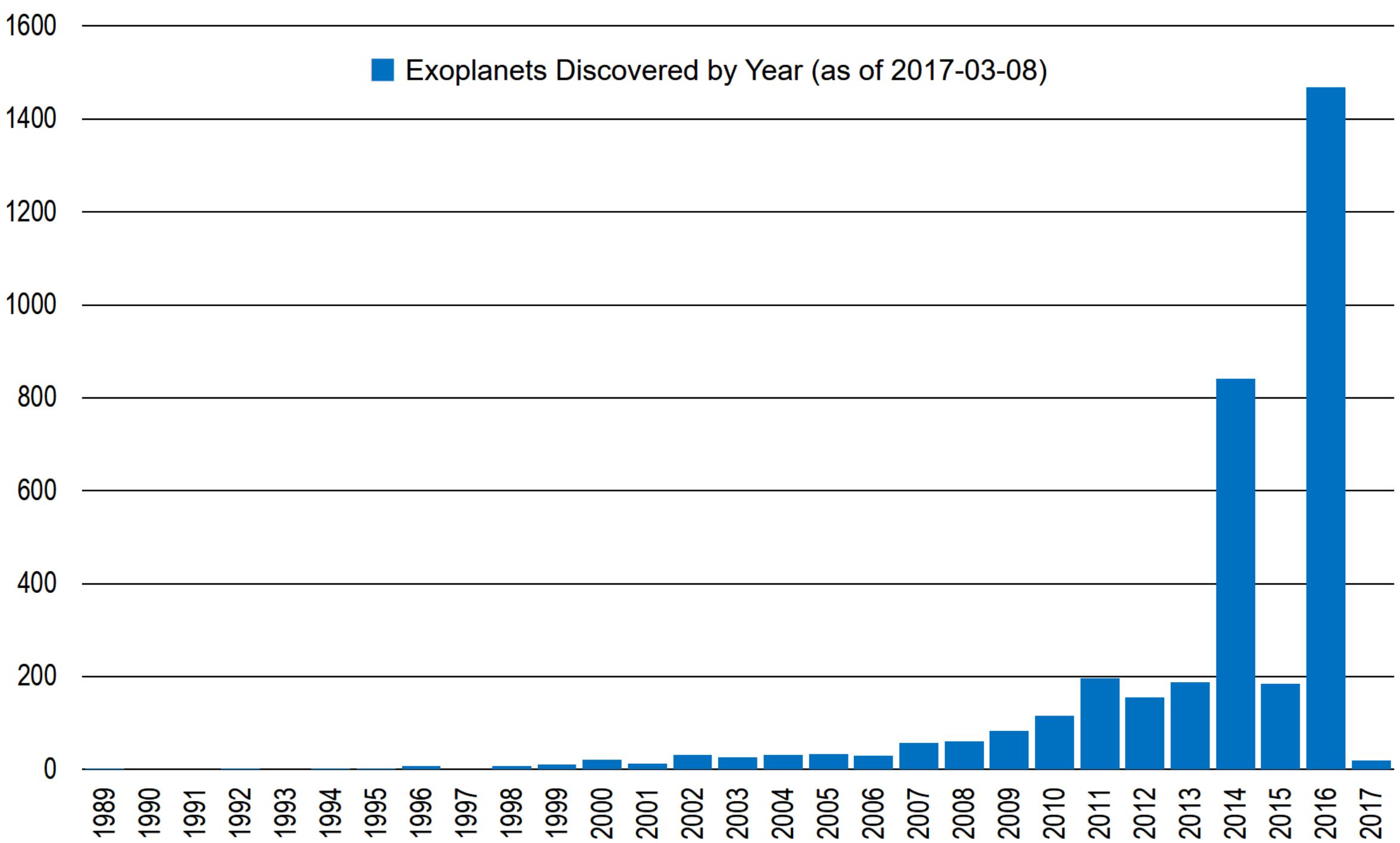
---

SERGEI POPOV

# Planets, brown dwarfs stars

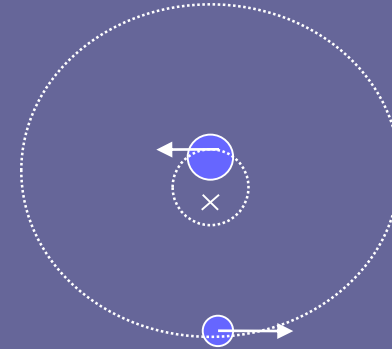
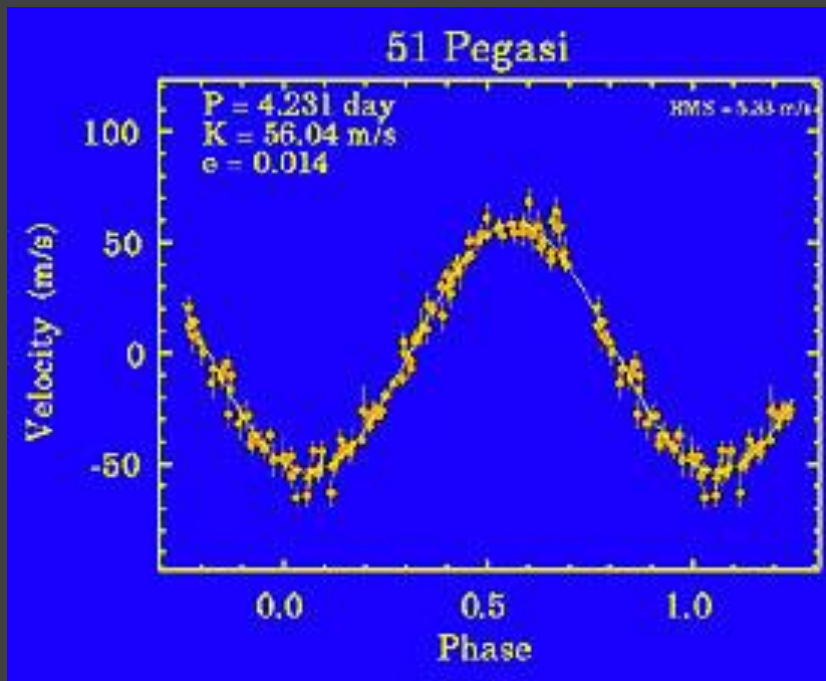


Brown dwarfs:  
(12-13)<M<(75-80)  
Jupiter masses

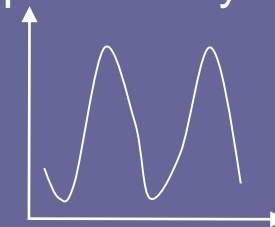


# Radial velocities

Michel Mayor and Didier Queloz 1995



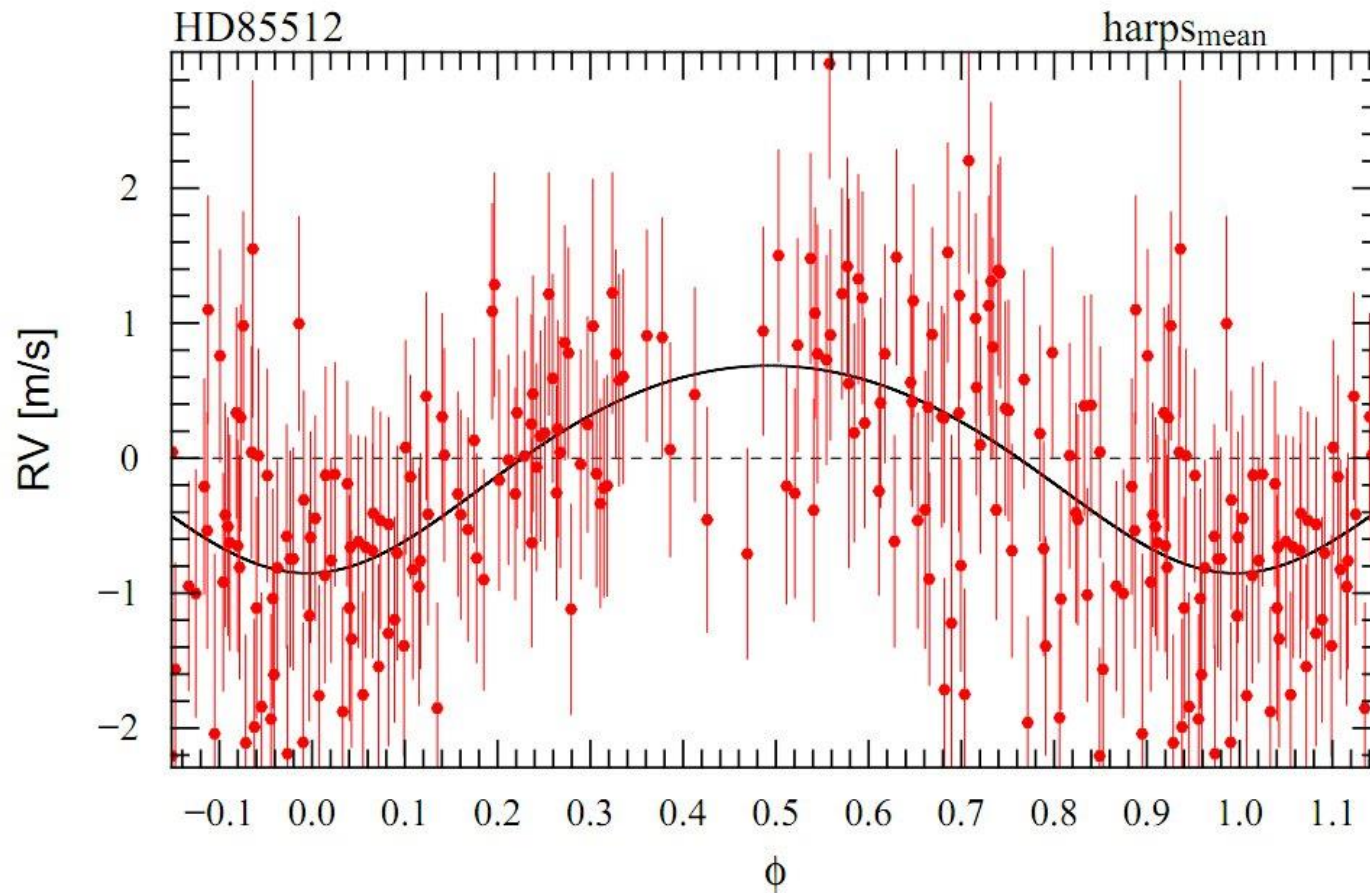
We see just the bright star.  
We measure that its radial velocity  
periodically changes.



Measure:

- Period
- Mass

# First light planets

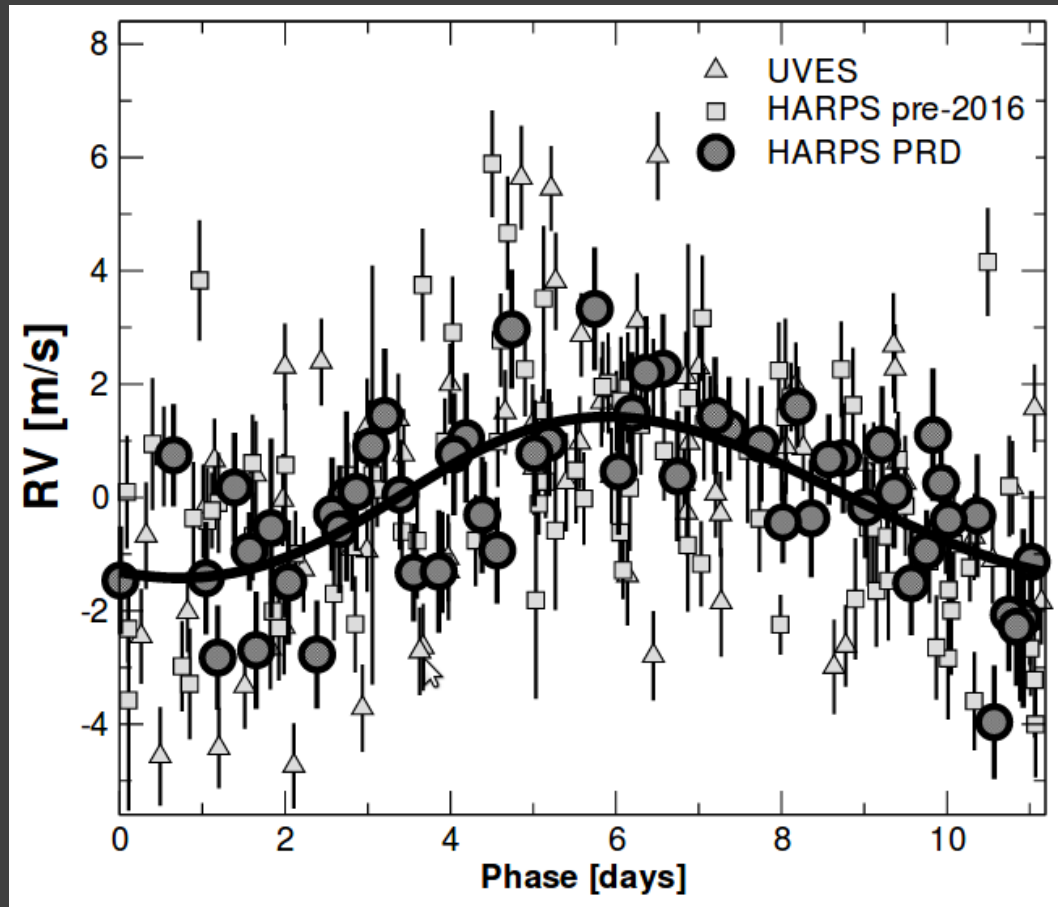


The problem is to measure small velocity variations for relatively long time.

Quality and stability of the spectrograph is more important than the telescope size.

This planet discovered by HARPS. Situated just near the zone of habitability.

# Proxima Centauri b



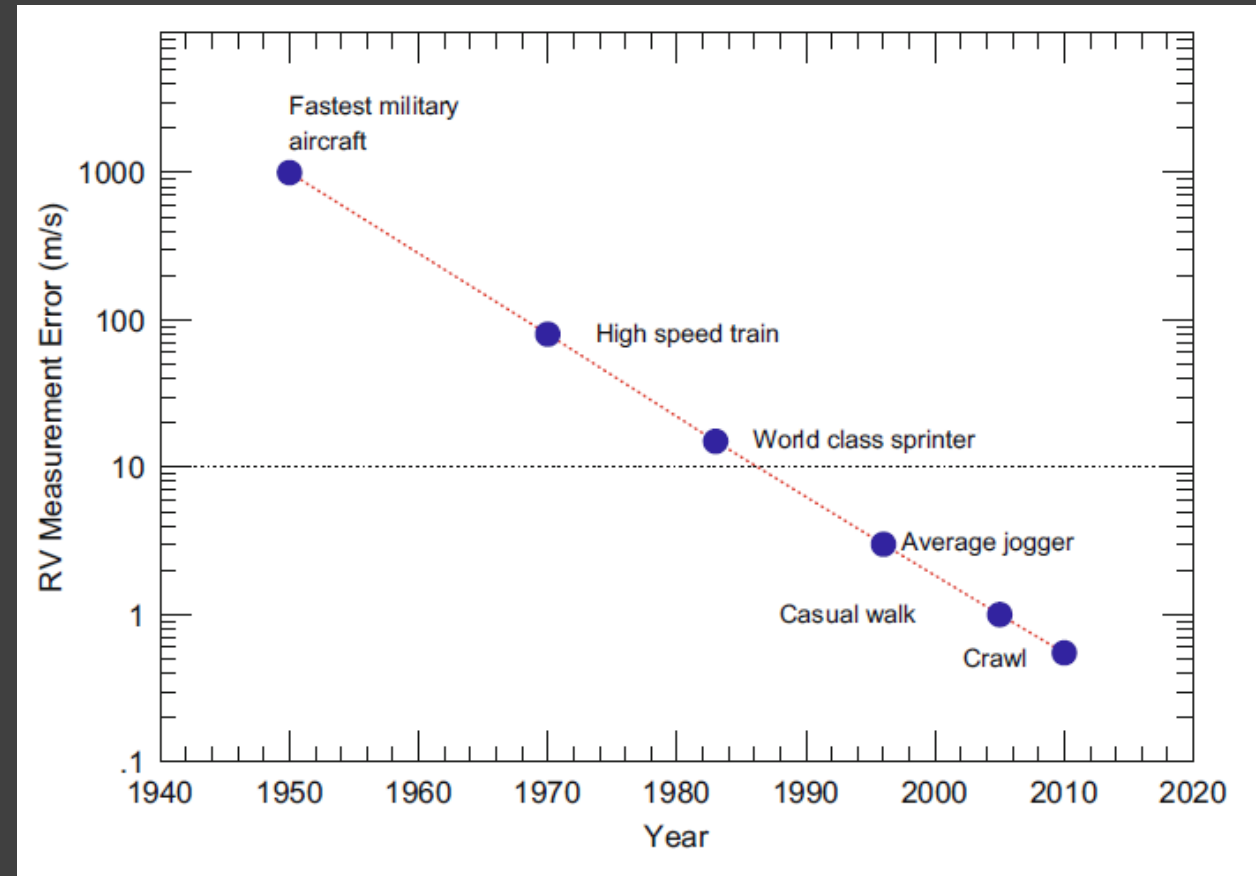
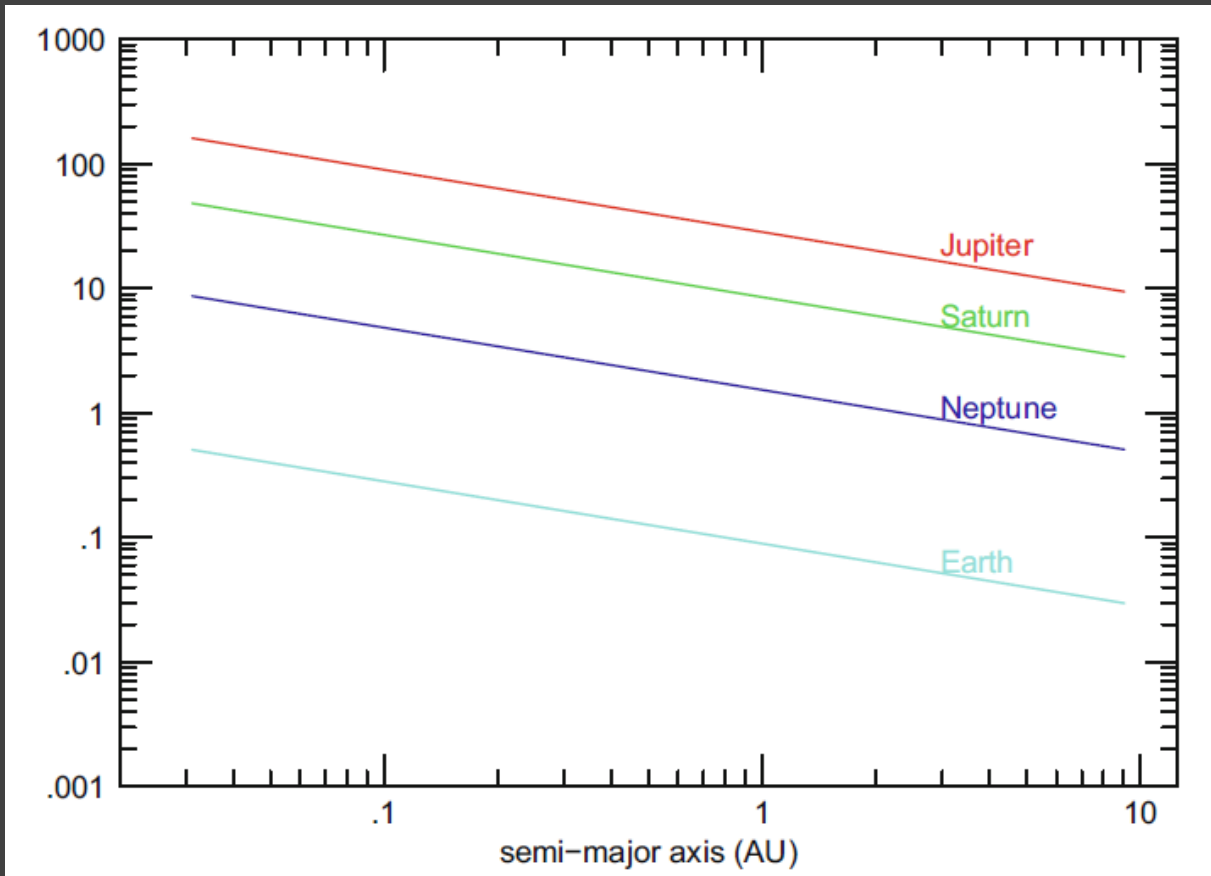
1.3 Earth masses

0.05 AU

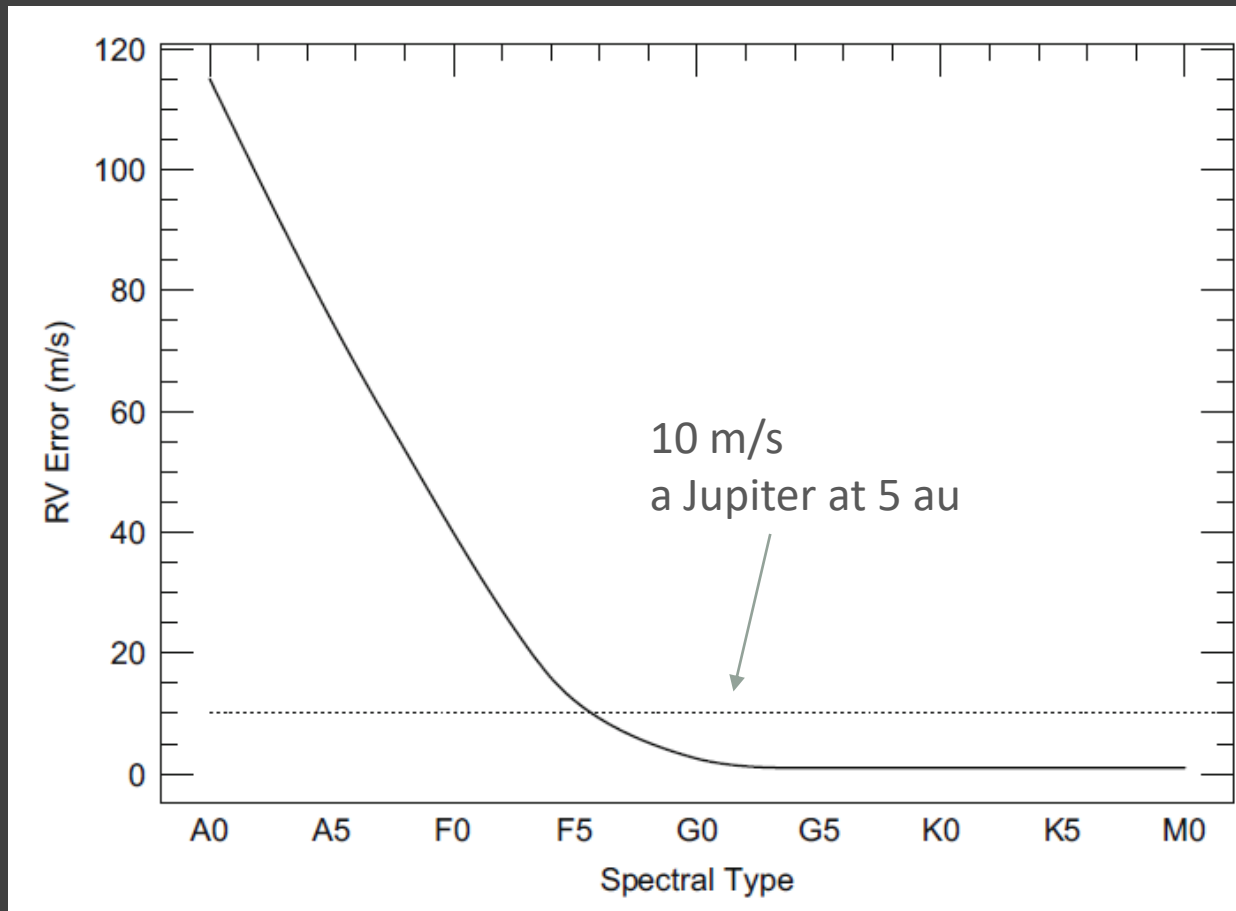
11 days

Habitability zone

# Radial velocities: data and measurements



# Role of a star



Difference is mainly due to

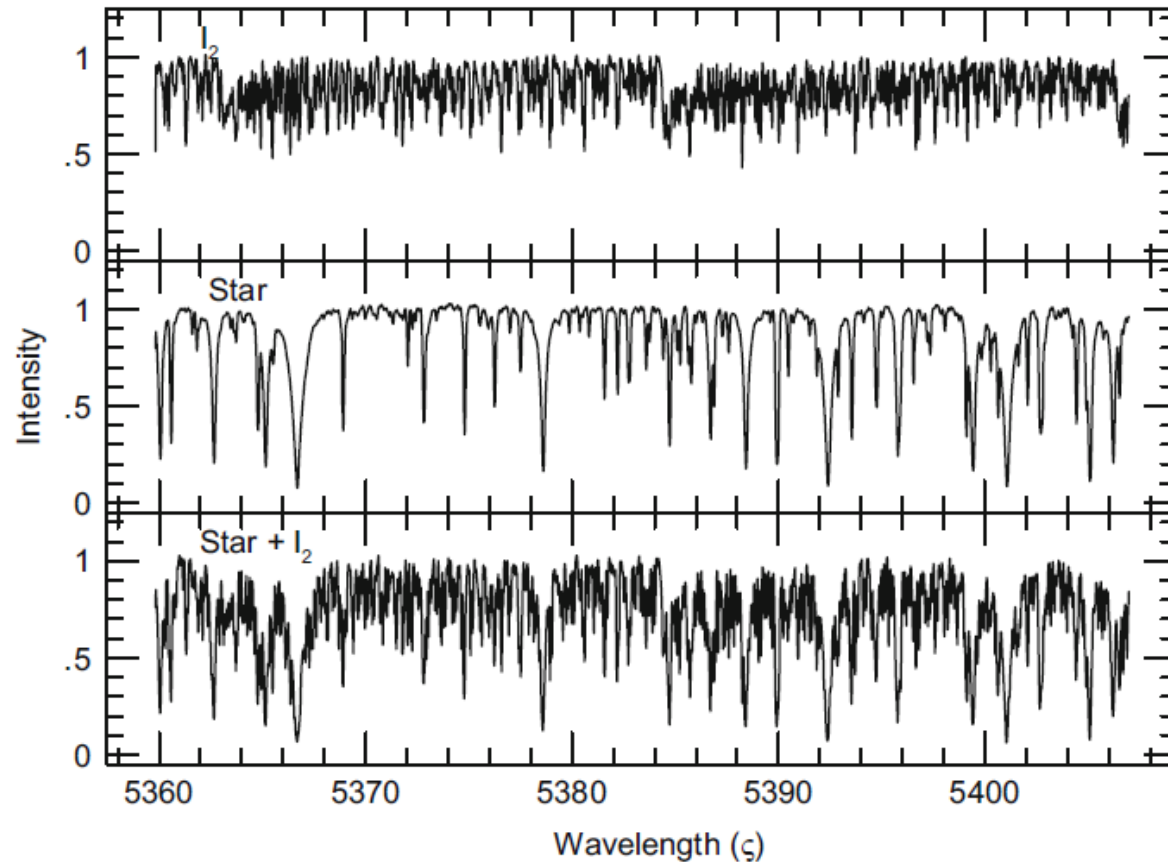
- Rapid rotation
- Smaller number of spectral lines

Without additional errors due to the instrument:

$$\sigma [\text{m/s}] = C(S/N)^{-1} R^{-3/2} B^{-1/2} (v \sin i / 2) f(\text{SpT})$$

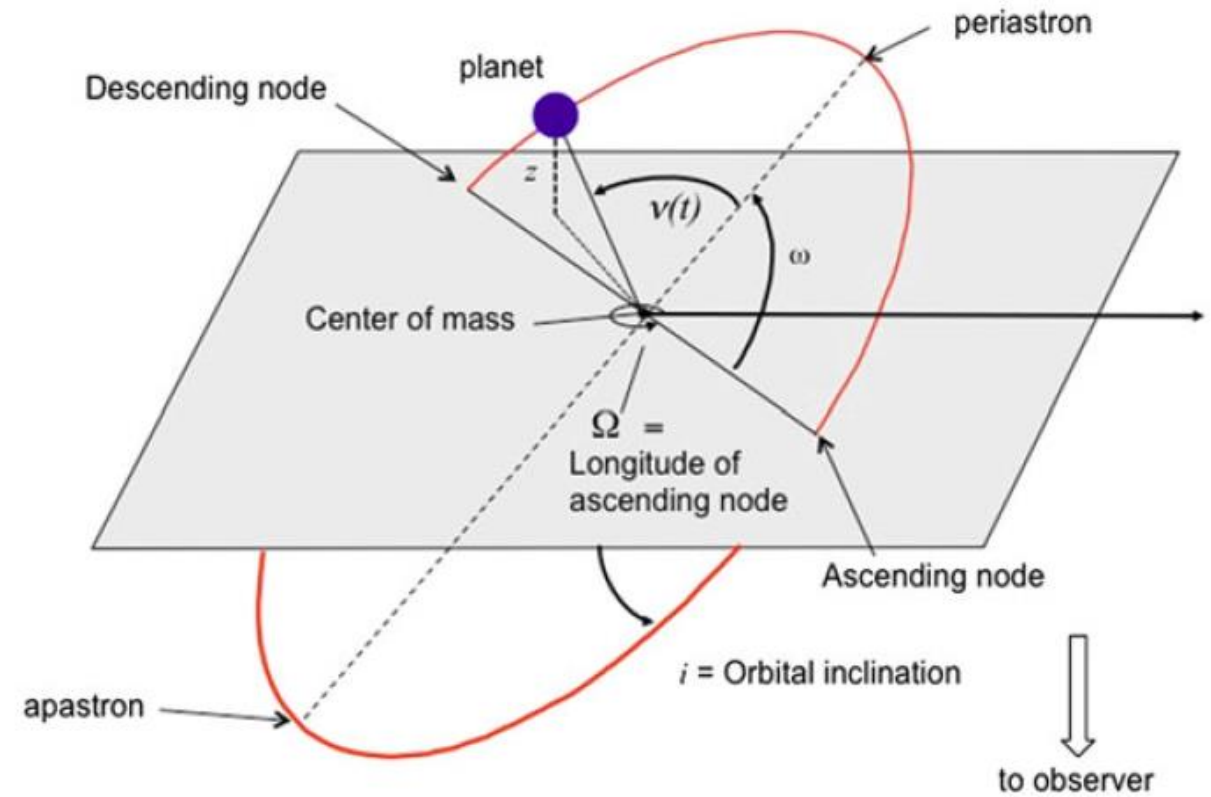
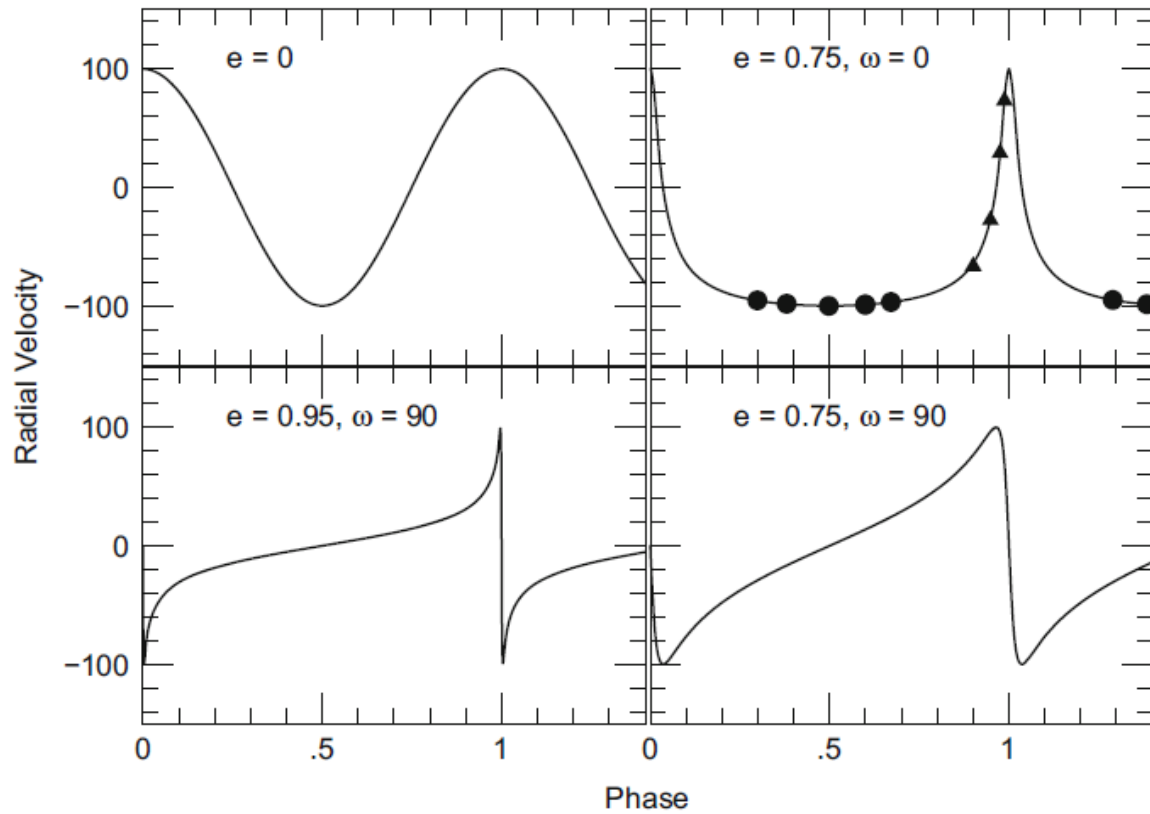


# Molecular iodine cell



$I_2$  cell became the first effective tool to provide lines for RV measurements.

# Velocity vs. phase for different orbits



# Planet mass

---

$$f(m) = \frac{M_2^3 \sin^3 i}{(M_1 + M_2)^2} = \frac{K_1^3 P (1 - e^2)^{3/2}}{2\pi G} \approx \frac{M_2^3 \sin^3 i}{M_1^2}$$

Thus, it is necessary to know the stellar mass ( $M_1$ )

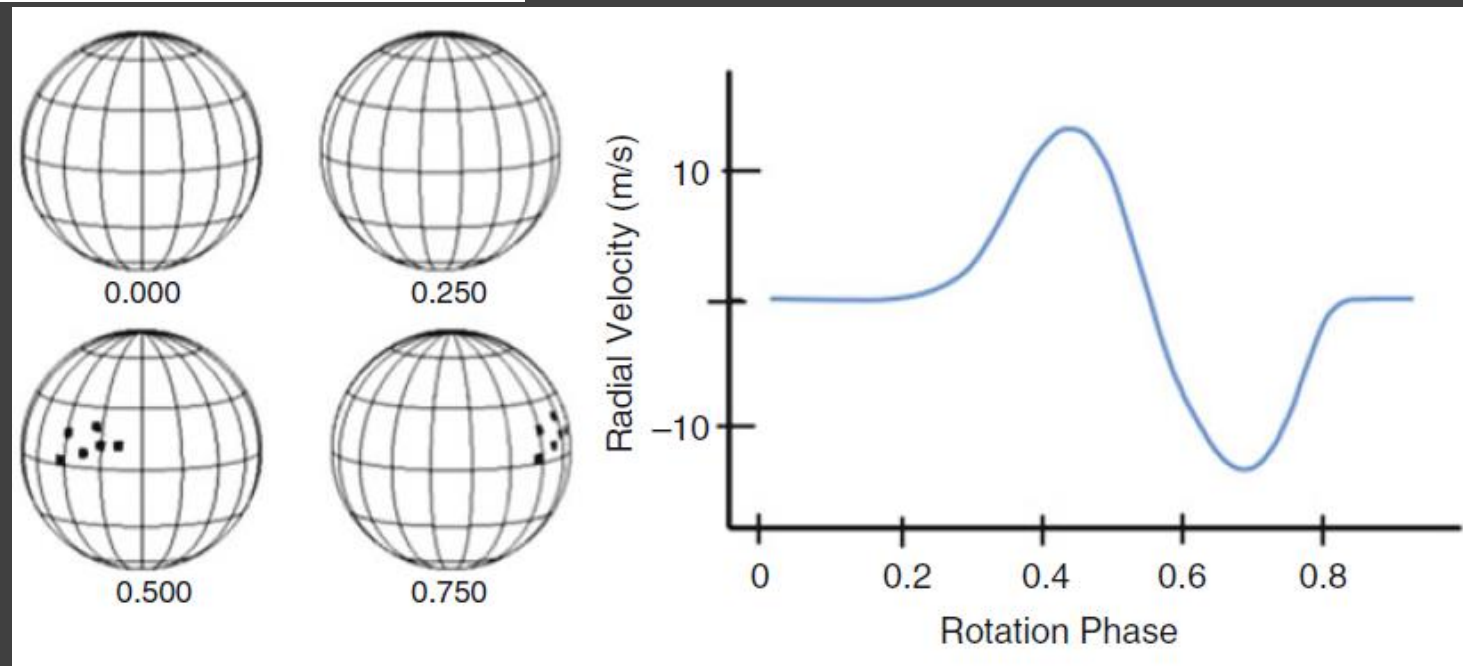
$$\langle \sin i \rangle = \frac{\int_0^\pi p(i) \sin i \, di}{\int_0^\pi p(i) \, di} = \frac{\pi}{4} = 0.79$$

For the mass function  
 $\langle \sin^3 i \rangle$  is important:

$$\frac{\int_0^\pi p(i) \sin^3 i \, di}{\int_0^\pi p(i) \, di} = 0.5 \int_0^\pi \sin^4 i \, di = \frac{3\pi}{16} = 0.59$$

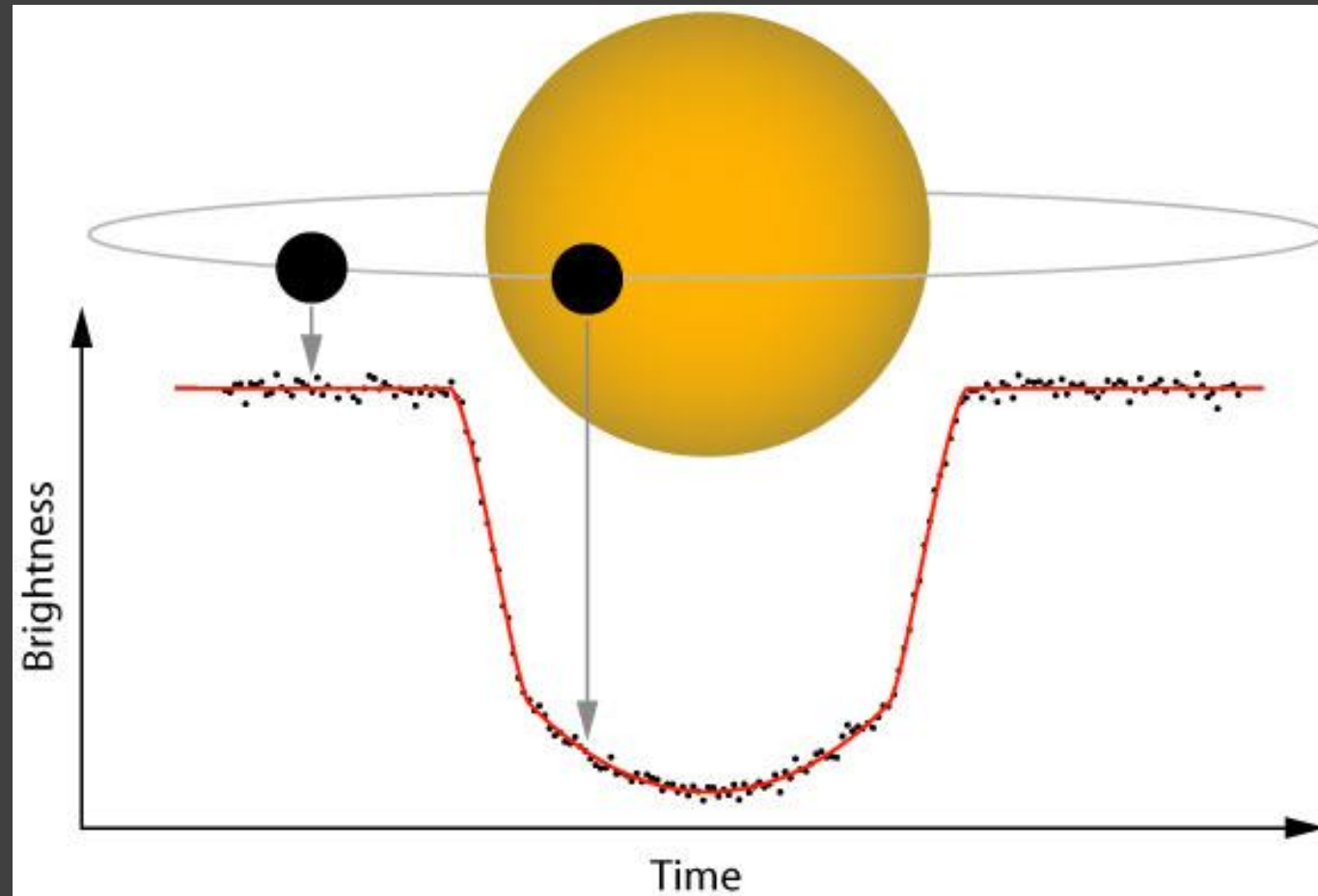
# Stellar noise

Phenomenon	RV amplitude ( $\text{m s}^{-1}$ )	Time scales
Solar-like oscillations	0.2–0.5	$\sim 5\text{--}15$ min
Stellar activity (e.g., spots)	1–200	$\sim 2\text{--}50$ days
Granulation/Convection pattern	$\sim$ few	$\sim 3\text{--}30$ years



# Planet transits

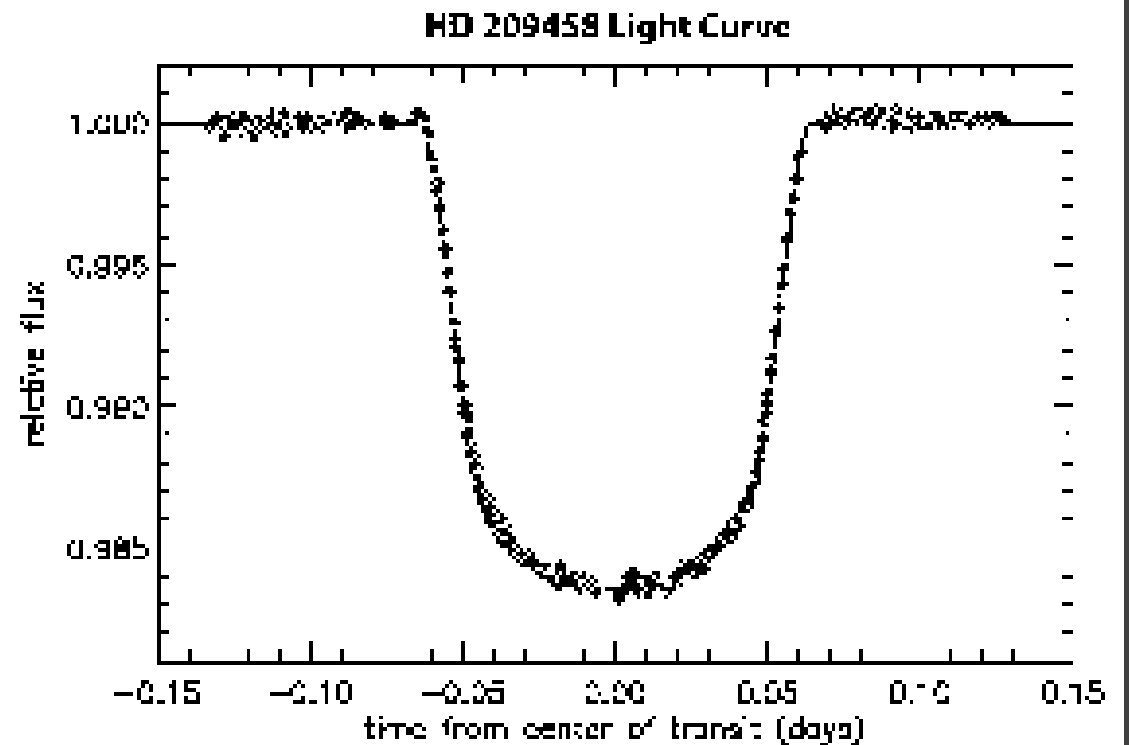
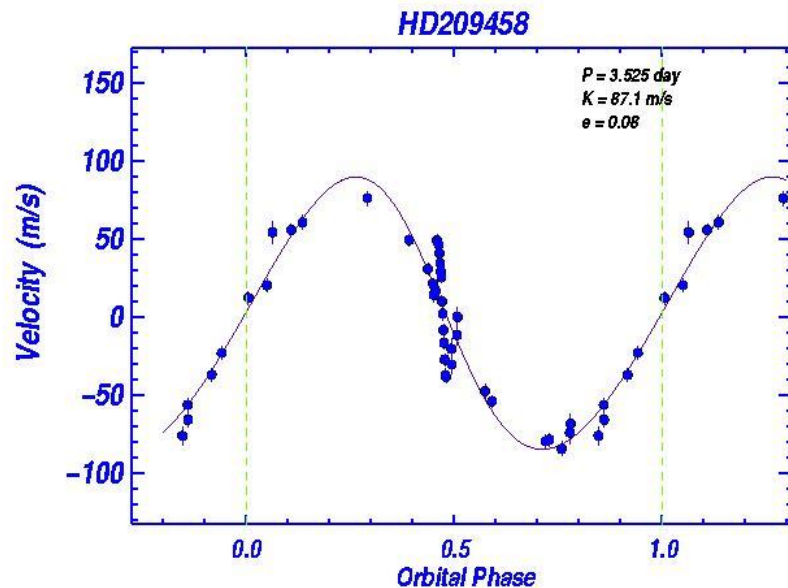
Proposed by  
Otto Struve  
in 1952



$$\frac{S_{\text{star}} - S_{\text{planet}}}{S_{\text{star}}}$$

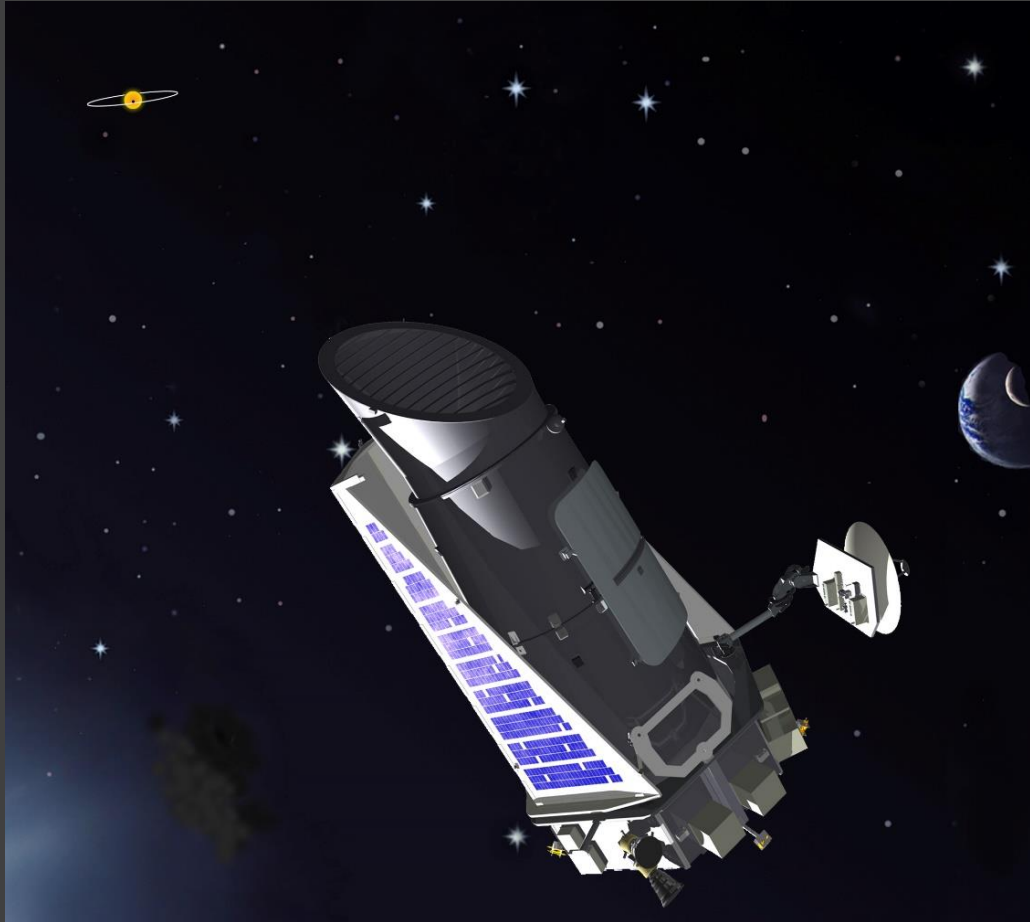
# The first transit measurement. HD 209458

The first measurements of a transit was made from the ground for a planet discovered by RV, and so known orbital parameters.



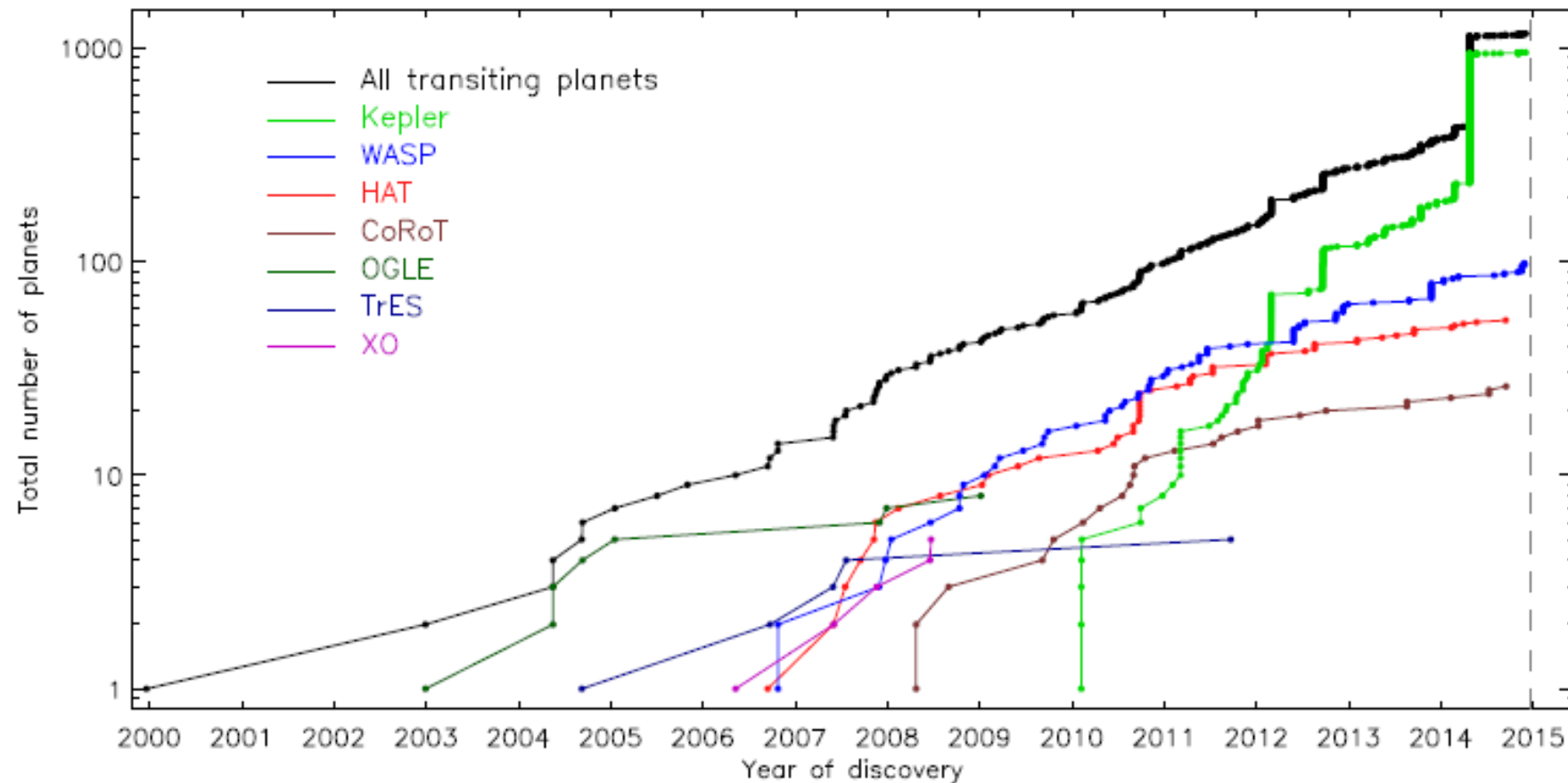
# Kepler and CoRoT

---



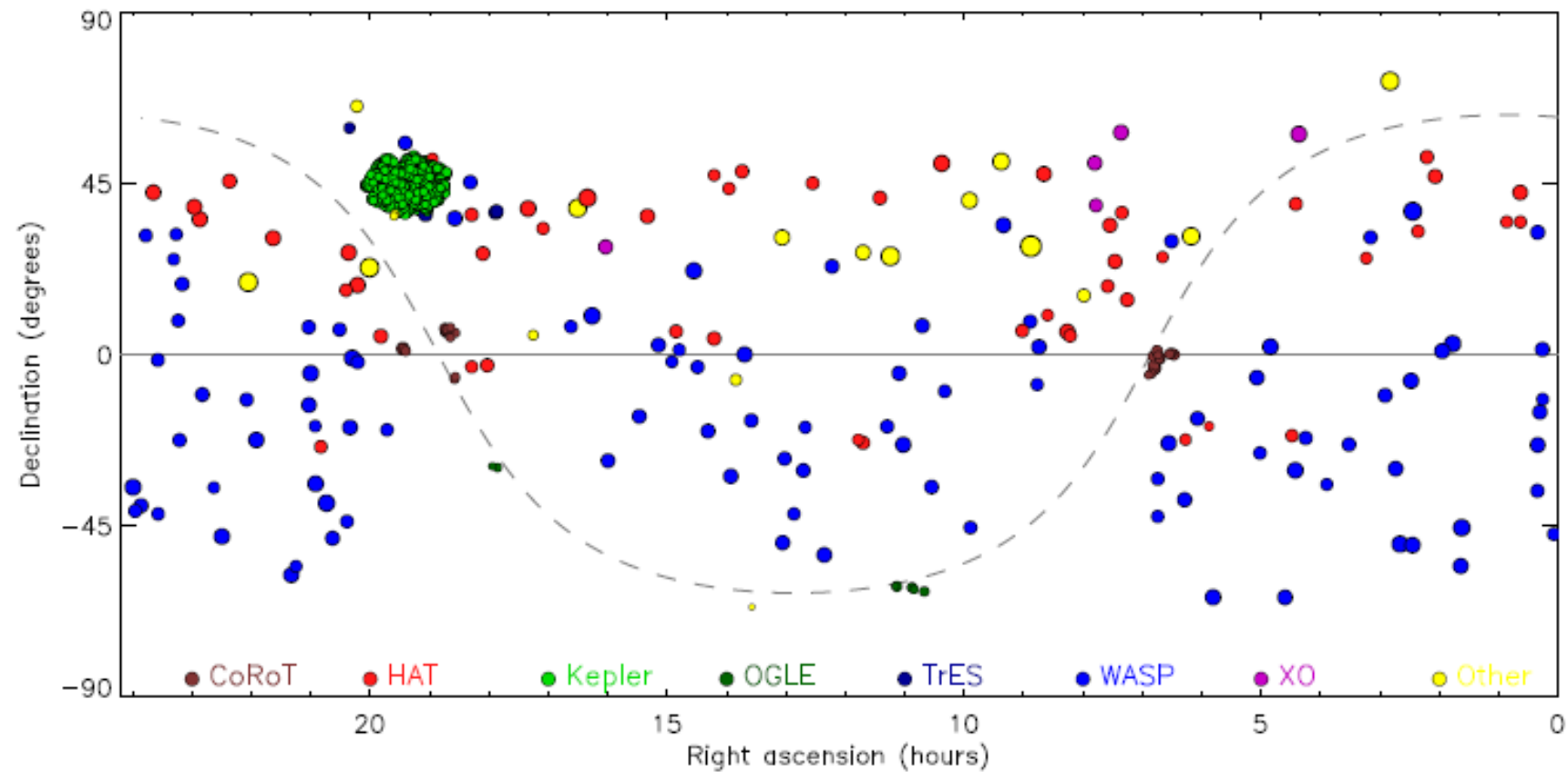


# Rate of discovery





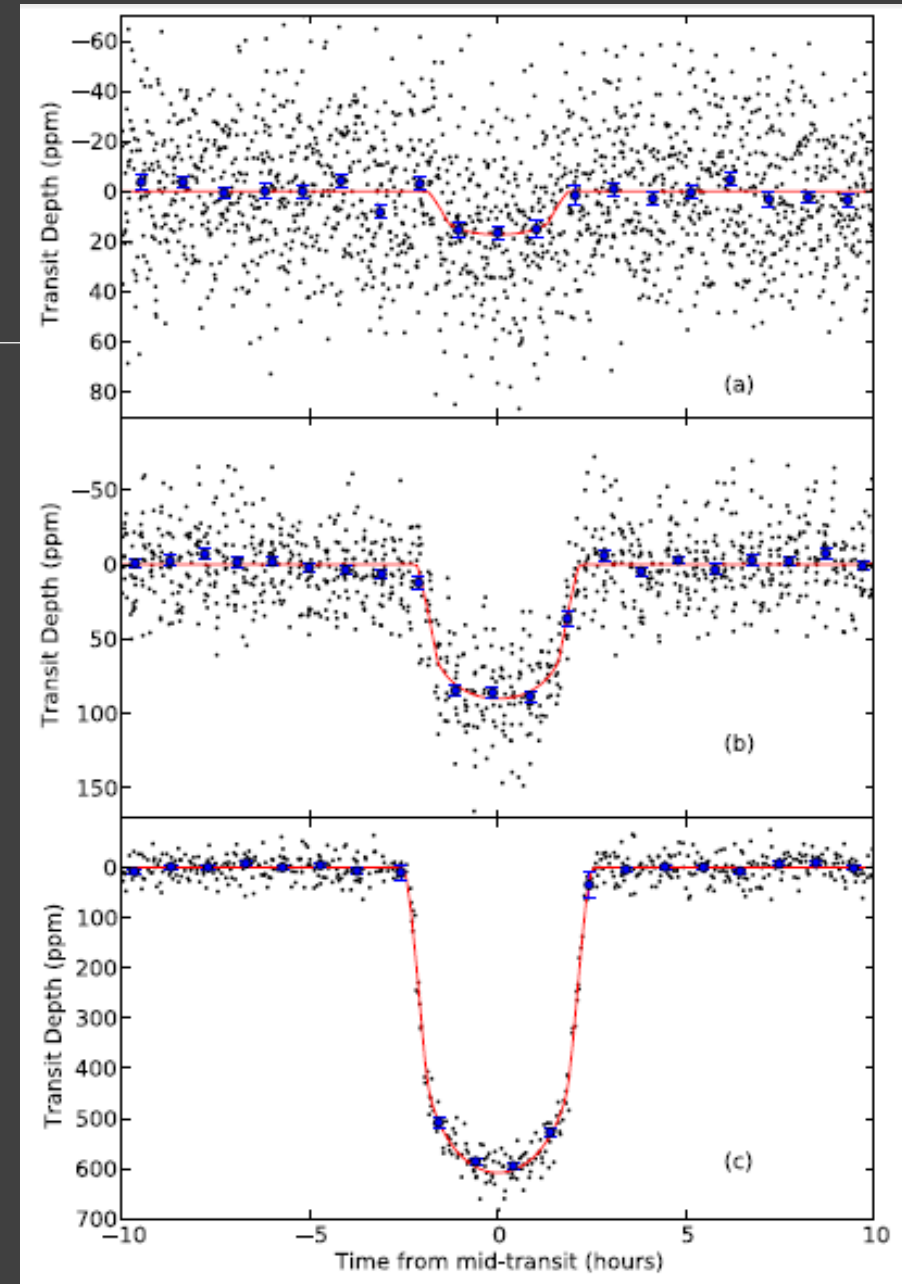
# Transiting planets in the sky



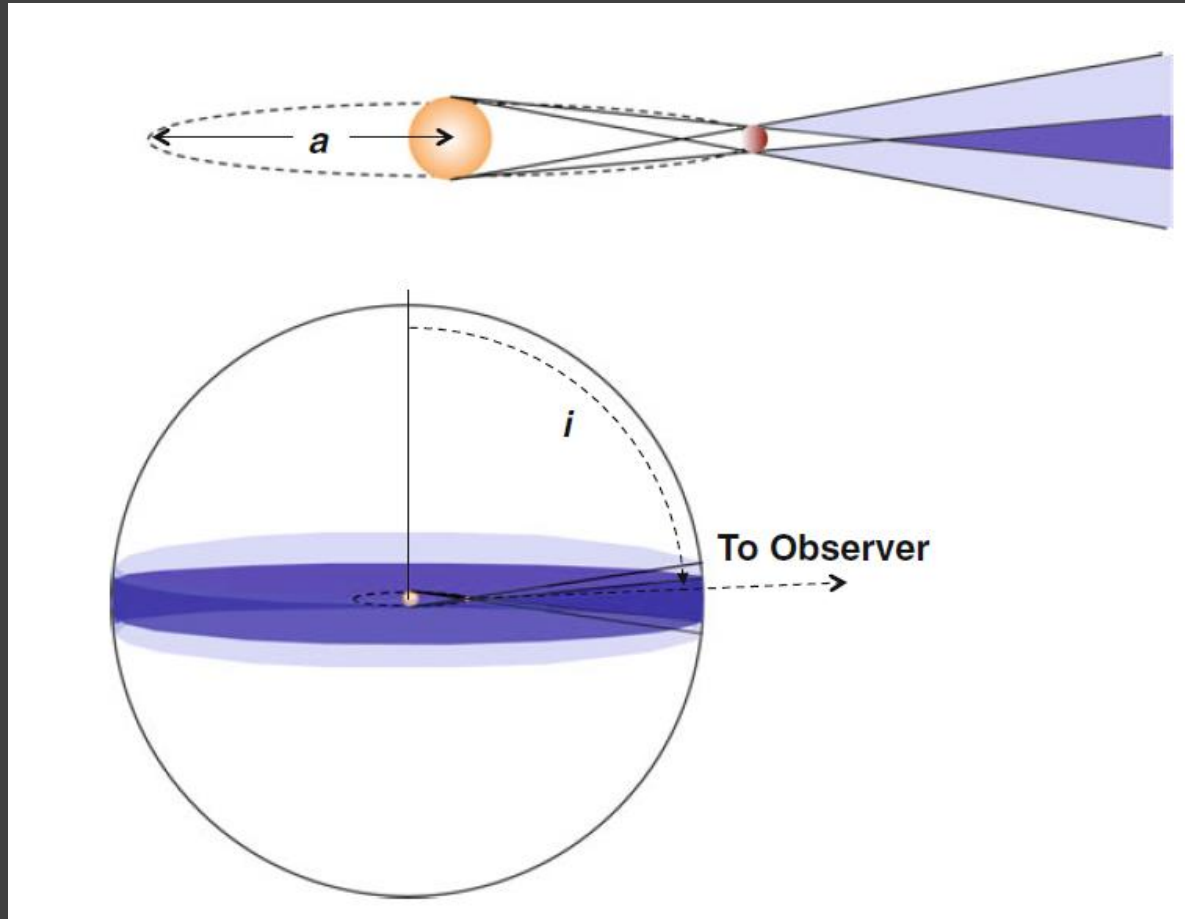
# Very small planets

Kepler-37b

The first discovered exoplanet  
with size smaller than Mercury

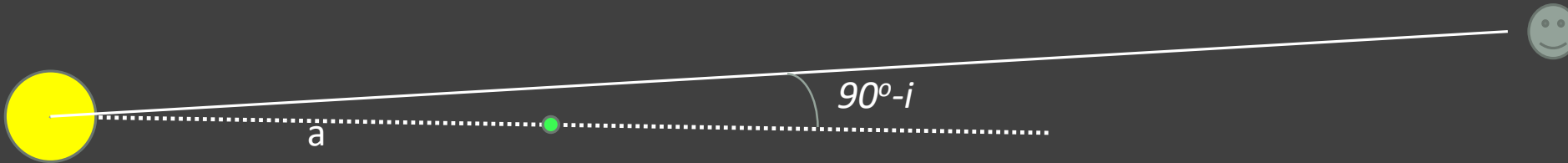


# Transit probability



$$\Pr \left( \cos i < \frac{R_*}{a} \right) \simeq 0.0046 \left( \frac{R_*}{R_\odot} \right) \left( \frac{1 \text{ au}}{a} \right).$$

# Transit conditions



$$b = \frac{a \cos i}{R_*}.$$

$$\frac{d\Omega}{4\pi} = \frac{2\pi \sin i \, di}{4\pi} = \frac{d(\cos i)}{2}.$$

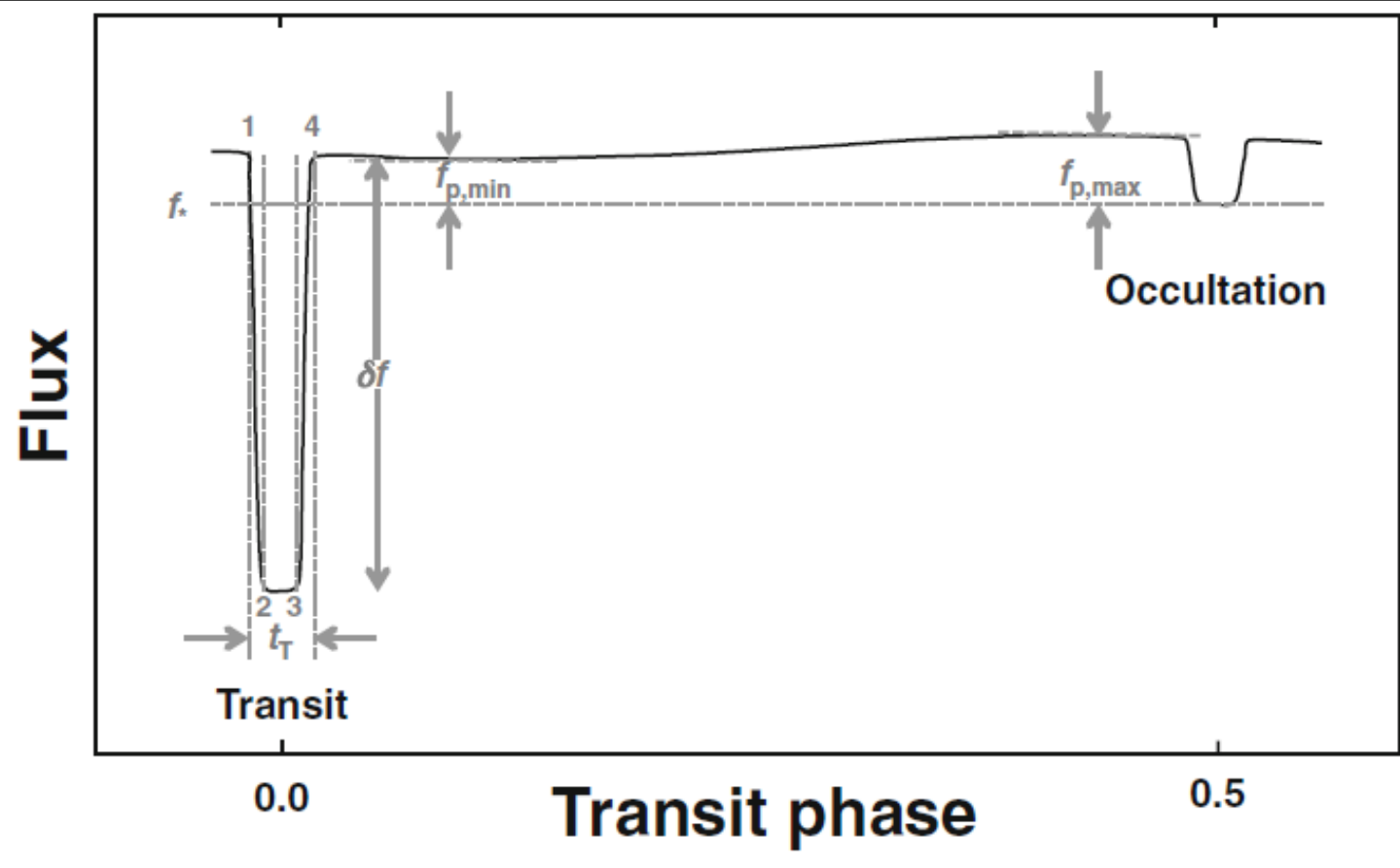
$$\Pr \left( \cos i < \frac{R_* + R_p}{a} \right) = \frac{1}{2} \int_{-(R_* + R_p)/a}^{(R_* + R_p)/a} = \frac{R_* + R_p}{a}.$$

$$R_p \ll R_*,$$

$$\Pr \left( \cos i < \frac{R_*}{a} \right) \simeq 0.0046 \left( \frac{R_*}{R_\odot} \right) \left( \frac{1 \text{ au}}{a} \right).$$

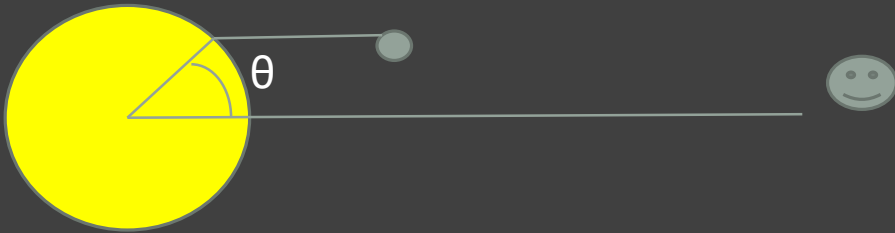
Selection in favour  
of close-in planets.

# Transit depth



$$\frac{\Delta f}{f} \simeq \left( \frac{R_p}{R_*} \right)^2 = 0.0105 \left( \frac{R_p}{R_{\text{Jup}}} \right)^2 \left( \frac{R_*}{R_{\odot}} \right)^{-2}$$

# Limb darkening



$$\mu = \cos \theta = \sqrt{1 - b^2}$$

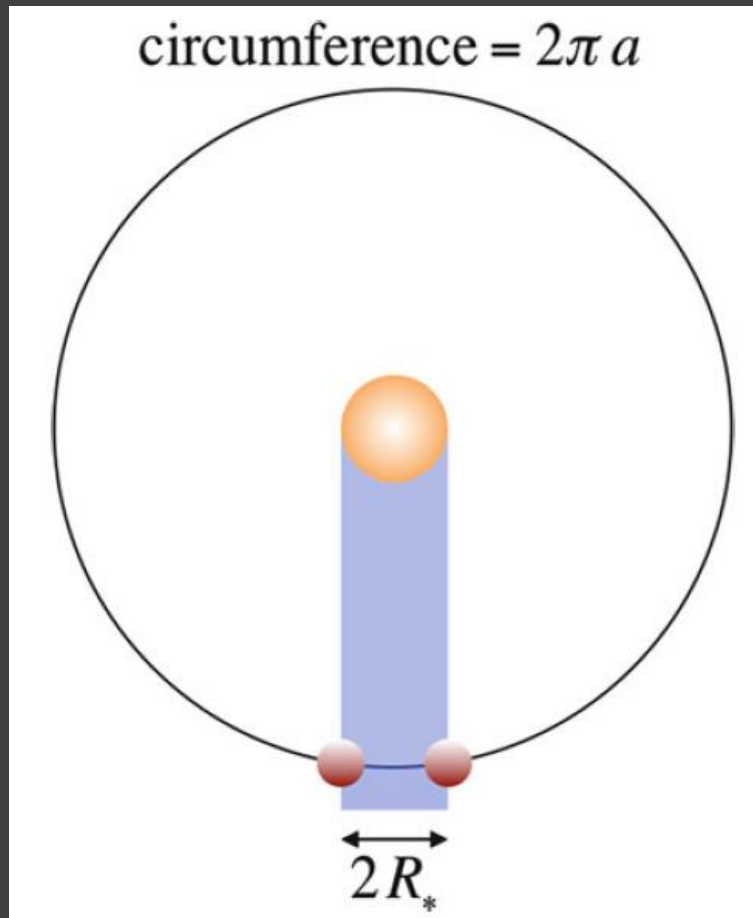
$$I = I_0(1 - u(1 - \mu))$$

Limb darkening can be taken into account in a more precise manner

$$\frac{I(\mu)}{I_0} = 1 - \sum_{n=1}^4 u_n(1 - \mu^{n/2}).$$

$$\begin{aligned} \frac{\Delta f}{f} &= \frac{\pi R_p^2 I_0 (1 - u + u \cos \theta)}{2\pi R_*^2 I_0 \int_0^{\pi/2} (1 - u + u \cos \theta) \sin \theta \cos \theta d\theta} \\ &= \frac{3(1 - u + u\sqrt{1 - b^2})}{3 - u} \left( \frac{R_p}{R_*} \right)^2. \end{aligned}$$

# Transit duration



$$\frac{T}{P} = \frac{1}{\pi} \sin^{-1} \frac{R_*}{a}$$

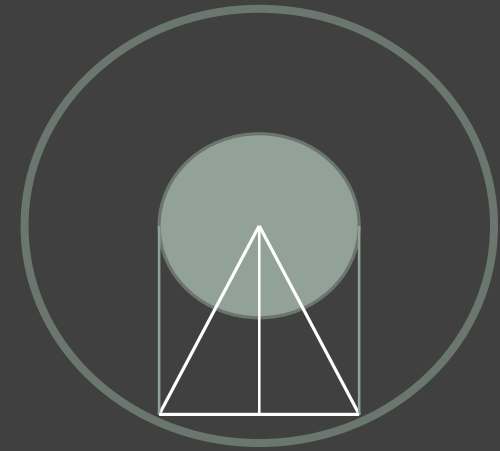
$$\frac{T}{P} = \frac{1}{\pi} \sin^{-1} R_* \left( \frac{4\pi^2}{GM_* P^2} \right)^{1/3}$$

$$\frac{t_T}{P} = \frac{1}{\pi} \sin^{-1} \left( \frac{R_*}{a} \left\{ \frac{[1 + (R_p/R_*)]^2 - [(a/R_*) \cos i]^2}{1 - \cos^2 i} \right\}^{1/2} \right)$$

$t_T$  – from first to last contact

For  $\cos i \ll 1$

$$\frac{t_T}{P} = \frac{R_*}{\pi a} \sqrt{\left(1 + \frac{R_p}{R_*}\right)^2 - b^2}.$$



# System parameters

---

$$T \simeq 3h \left( \frac{P}{4d} \right)^{1/3} \left( \frac{\rho_*}{\rho_\odot} \right)^{-1/3}$$

Stellar density estimate

$$\frac{dv_r}{dt} = \frac{2\pi K}{P} = \frac{GM_p}{a^2} = g_p \frac{R_p^2}{a^2} = g_p \frac{R_p^2}{R_*^2} \frac{R_*^2}{a^2},$$

K – stellar velocity

$$g_p = \frac{2\pi K}{P} \left( \frac{R_*}{R_p} \right)^2 \left( \frac{a}{R_*} \right)^2$$

Planet density

$$\rho_p = \frac{3g_p}{4\pi GR_p} = \frac{3g_p}{4\pi GR_*} \left( \frac{R_*}{R_p} \right)$$

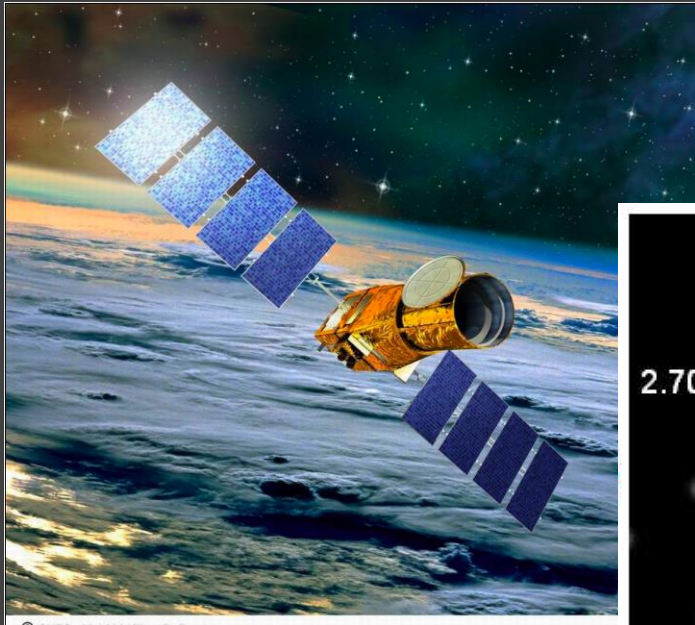
$$R_* = \theta d = \theta / \hat{\pi}:$$

$$\rho_p = \frac{3g_p \hat{\pi}}{4\pi G\theta} \left( \frac{R_*}{R_p} \right)$$

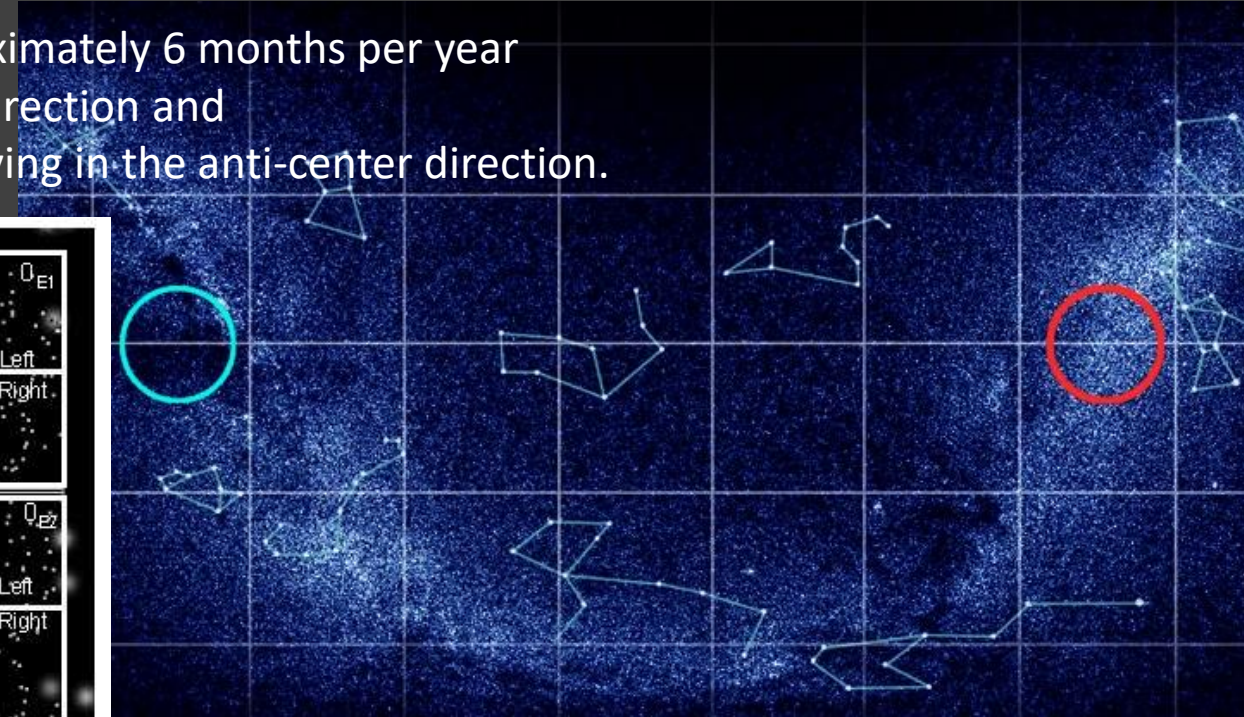
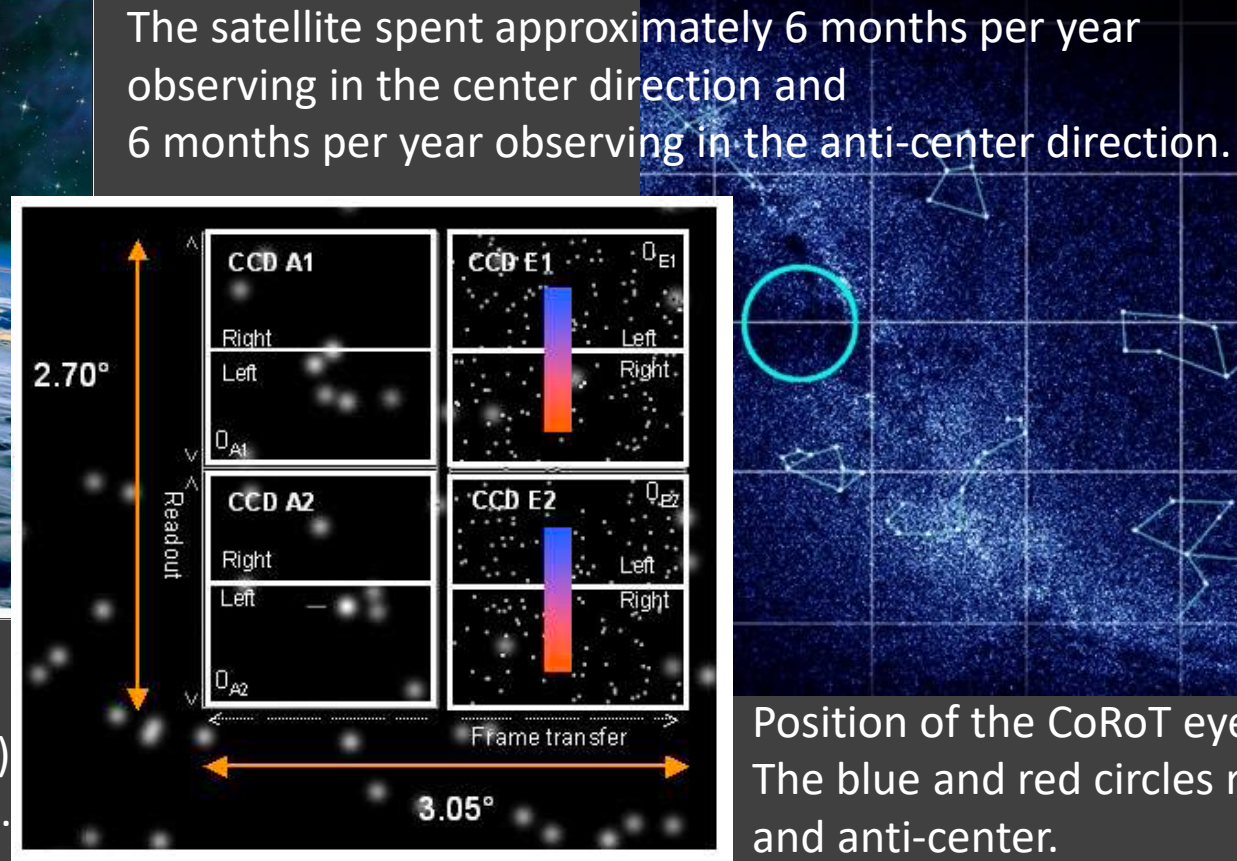


# CoRoT

December 2006 – November 2012  
27-cm telescope



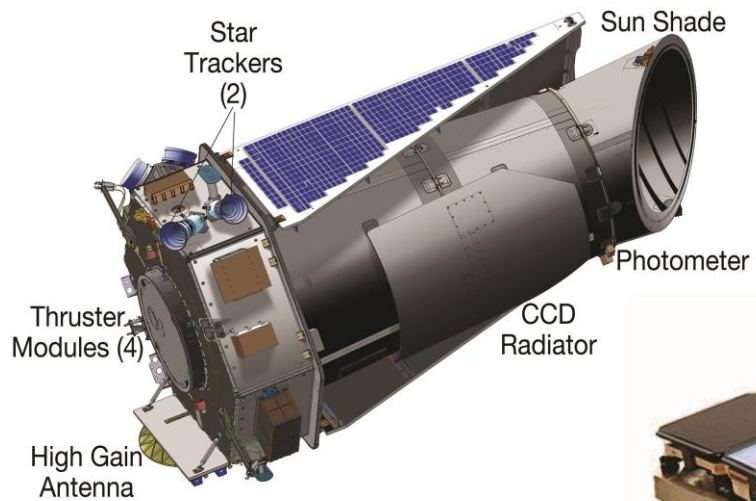
Focal planet arrangement  
of the asteroseismology (A1, A2)  
and the exoplanet (E1, E2) CCDs.



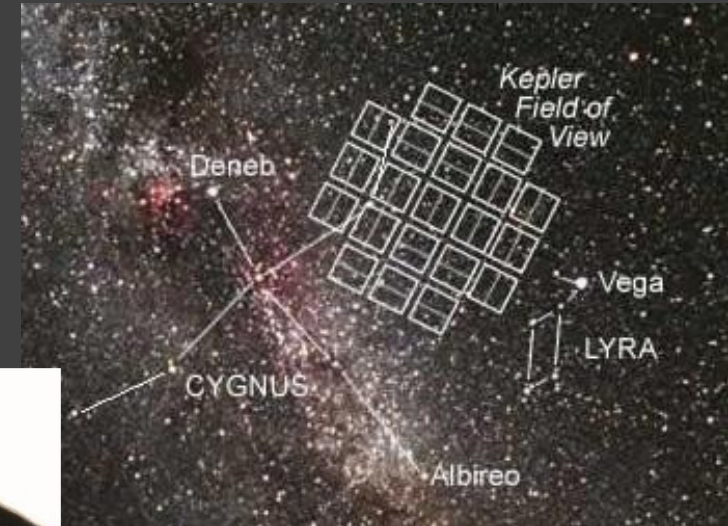
Position of the CoRoT eyes in the sky.  
The blue and red circles represent the center  
and anti-center.

# Kepler

2009-2013 + K2-mission  
0.95 m telescope



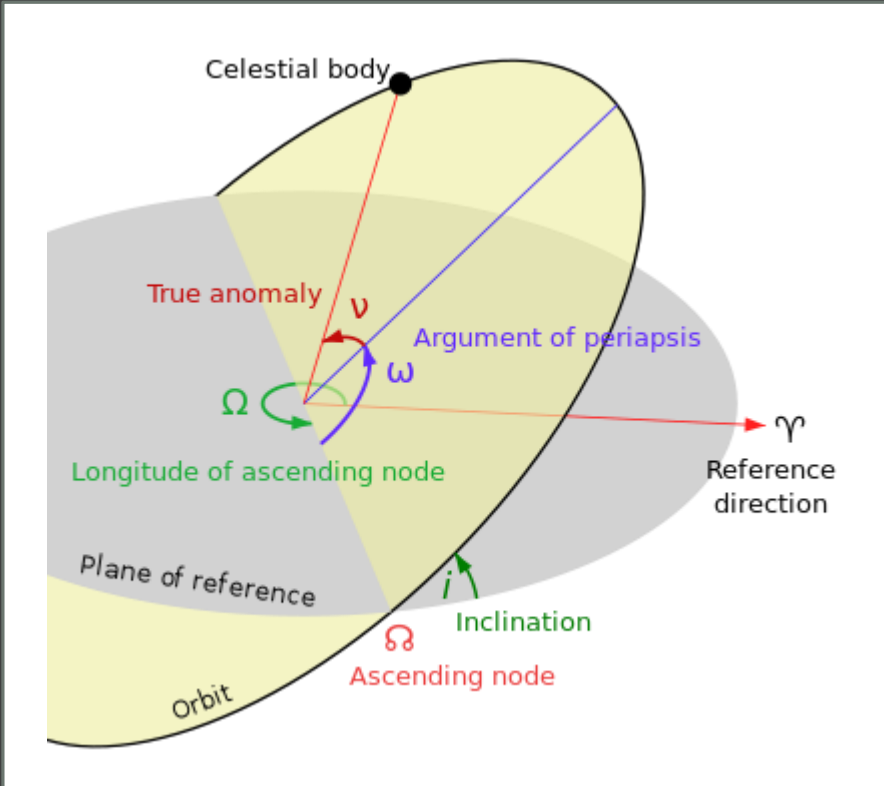
Monitoring of ~150 000 stars



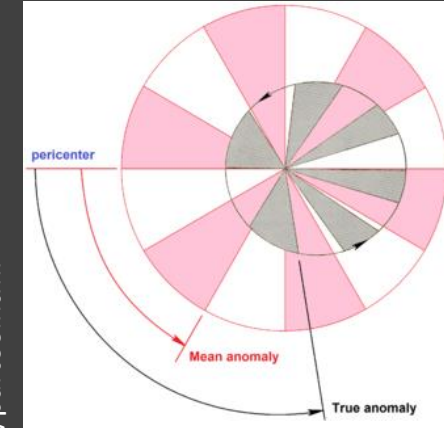
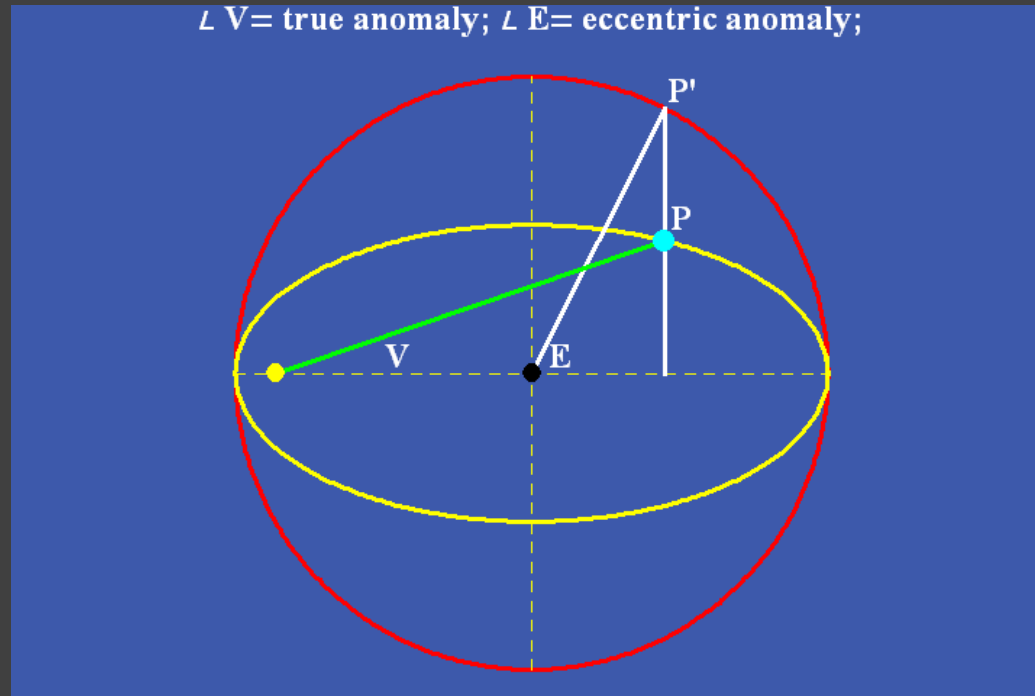
Field of view ~115 sq. degrees



# Orbital elements



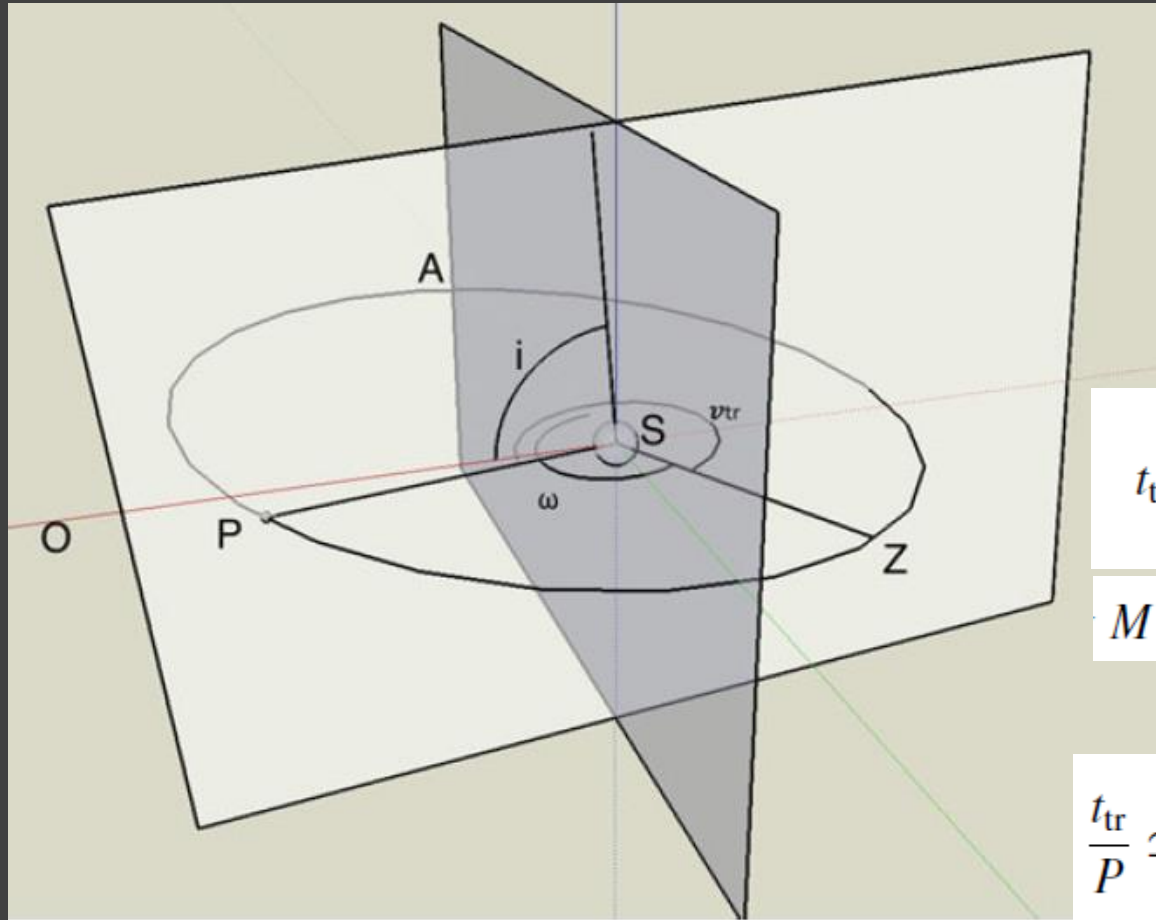
$\nu$  – true anomaly  
 $\omega$  – argument of periastron  
 $E$  - eccentric anomaly  
 $M$  – mean anomaly



<http://www.wlym.com/antidummies/part66.html>

$$z=d/R_{\text{star}}$$

$$p = R_p / R_{\text{star}}$$



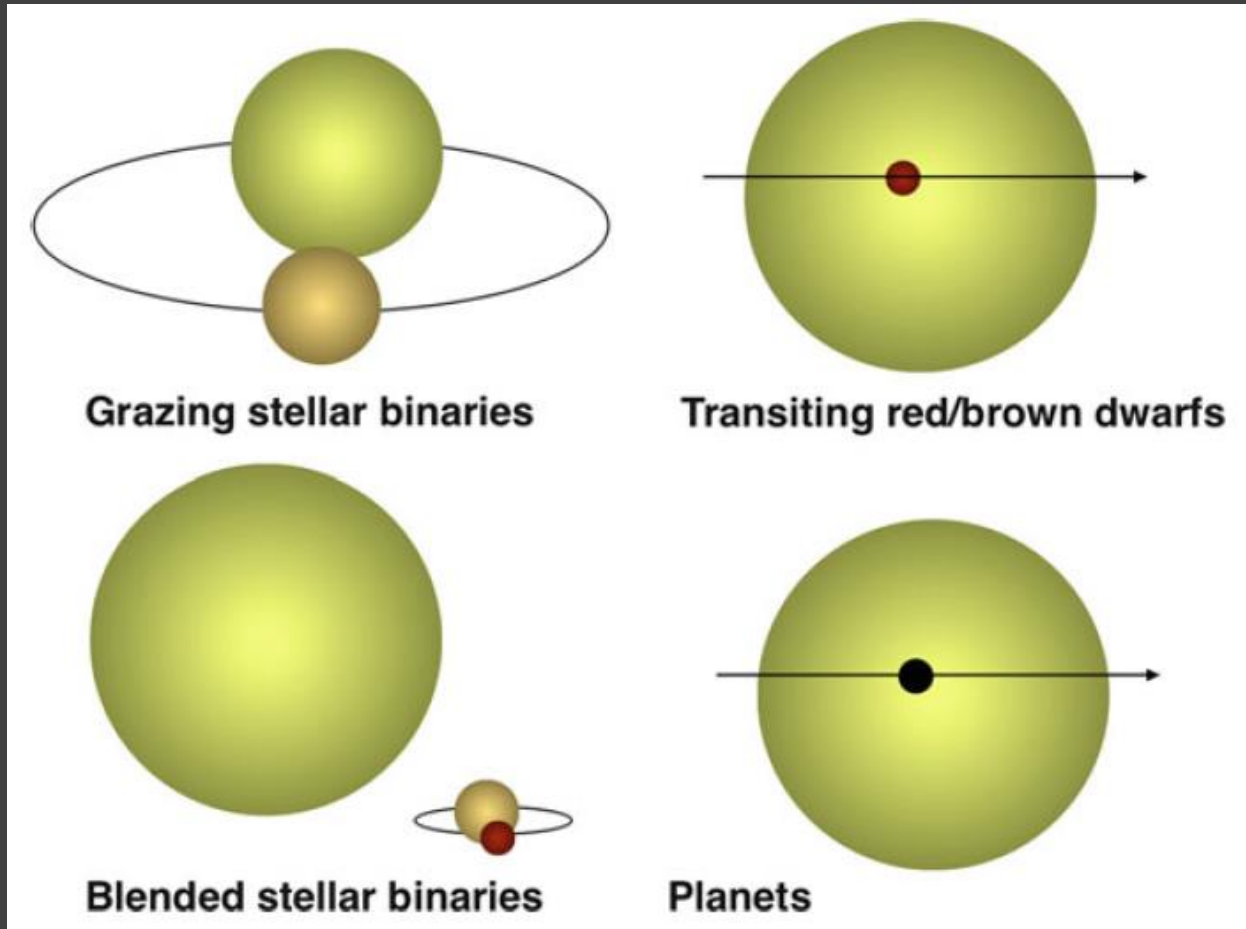
$$v_{\text{occ}} = \frac{3\pi}{2} - \omega,$$

$$t_{\text{tr}} - t_0 = \frac{P}{2\pi} M_{\text{tr}} = \frac{P}{2\pi} (E_{\text{tr}} - e \sin E_{\text{tr}}).$$

$$E_1 = M,$$

$$\frac{t_{\text{tr}}}{P} \simeq \frac{R_*}{a} \frac{\sqrt{(1 + R_p/R_*)^2 - b^2}}{\pi} \frac{1 + e \sin \omega}{1 - e^2}.$$

# Transits and transit-like events



# Spectral lines and planet/star mass ratio

$$\dot{v}_r \simeq \frac{GM_*}{a^2} = \frac{2\pi K}{P} \frac{M_*}{M_p}.$$

Observations of spectral line in the planet atmosphere can allow to measure important parameters of the system!

Measurements of the radial acceleration (due to observations of spectral lines in the planet atmosphere) allow to measure stellar mass.

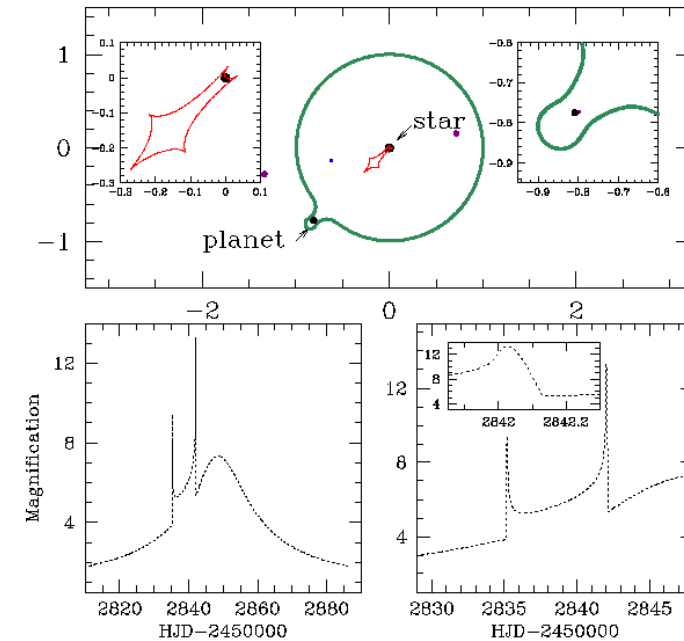
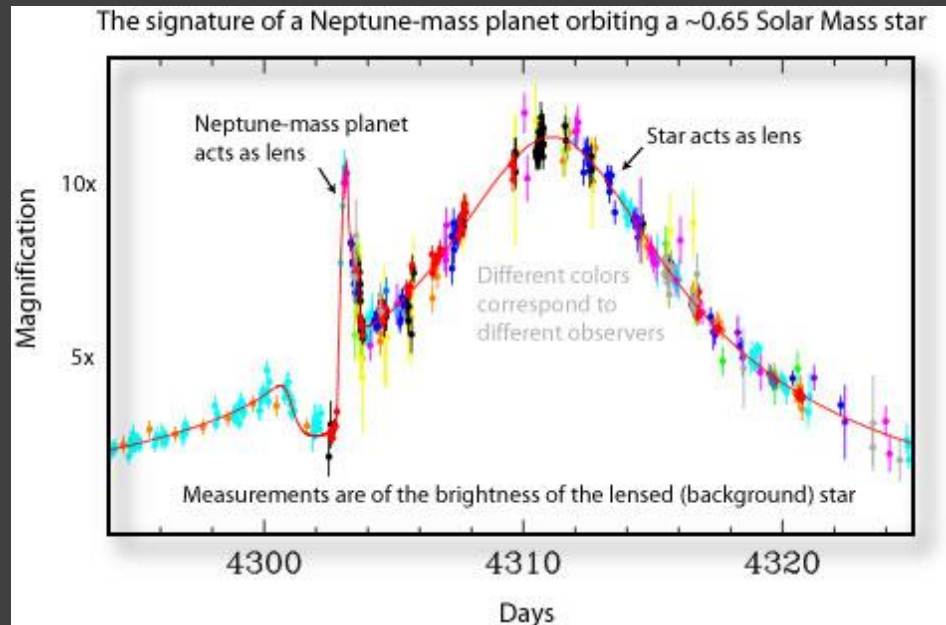
$$\frac{T}{P} = \frac{1}{\pi} \sin^{-1} \frac{R_*}{a}$$

$$\delta v_r \simeq \frac{P}{\pi} \frac{R_*}{a} \frac{2\pi K}{P} \frac{M_*}{M_p}.$$

If narrow spectral lines in the planet atmosphere can be observed during transit then it is possible to derive  $M_{\text{star}}/M_{\text{planet}}$

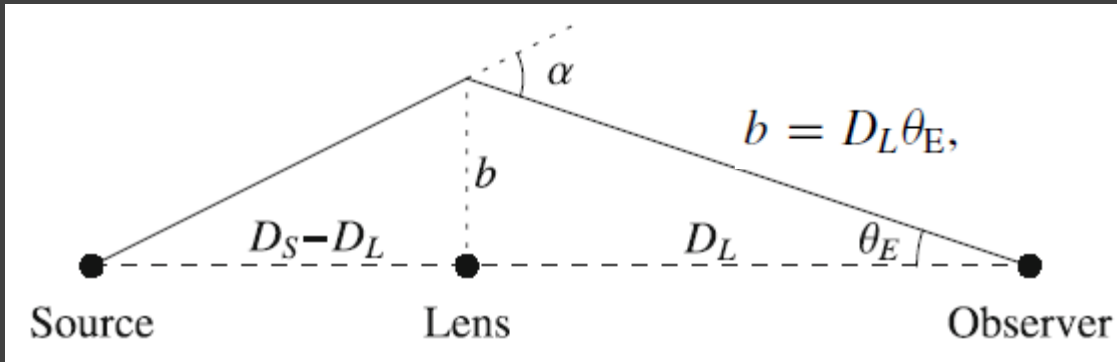
# Exoplanet detection via microlensing

- Sensitive to low mass planets (down to  $0.1 M_{\text{earth}}$ )
- Sensitive to wide orbits (1-4 AU)
- Sensitive to free-floating planets



<https://www3.nd.edu/~bennett/ma53-ogle235/technical.gif>

# Gravitational microlensing - 1



Probability of microlensing is small.  
For stars it is  $\sim 10^{-5} - 10^{-6}$  per year.  
For planets it is lower, as  $\theta_E \sim M^{1/2}$   
and  $M_{\text{planet}}/M_{\text{star}} \sim 10^{-4}$

$$\alpha = b/D_L + b/(D_S - D_L).$$

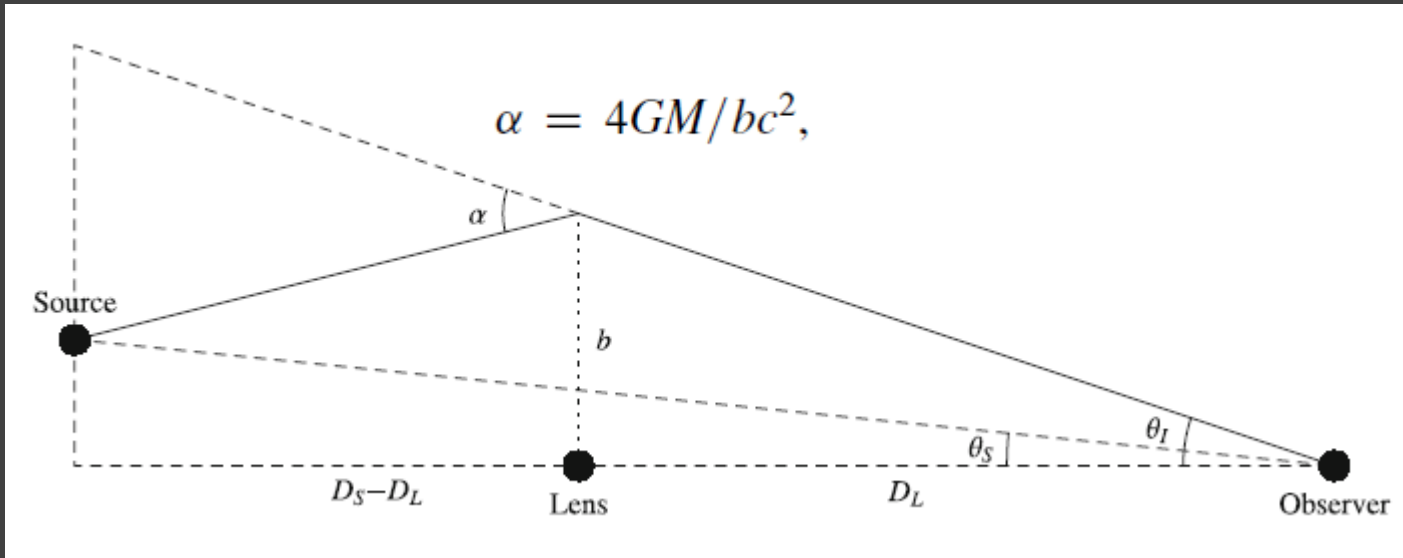
$$\theta_E = \sqrt{\kappa M \pi_{\text{rel}}}; \quad \kappa \equiv \frac{4G}{c^2 \text{AU}} \simeq 8.14 \frac{\text{mas}}{M_{\odot}},$$

$$\pi_{\text{rel}} = \text{AU}(D_L^{-1} - D_S^{-1})$$

$$\tau = \int dD_L \pi (D_L \theta_E)^2 n(D_L) \sim \frac{4\pi G M n}{c^2} D^2 = \frac{4\pi G \rho}{c^2} D^2 \sim \frac{G M_{\text{tot}}}{D c^2} \sim \frac{v^2}{c^2}$$



# Gravitational microlensing - 2



$$(\theta_I - \theta_S)D_S = \alpha(D_S - D_L)$$

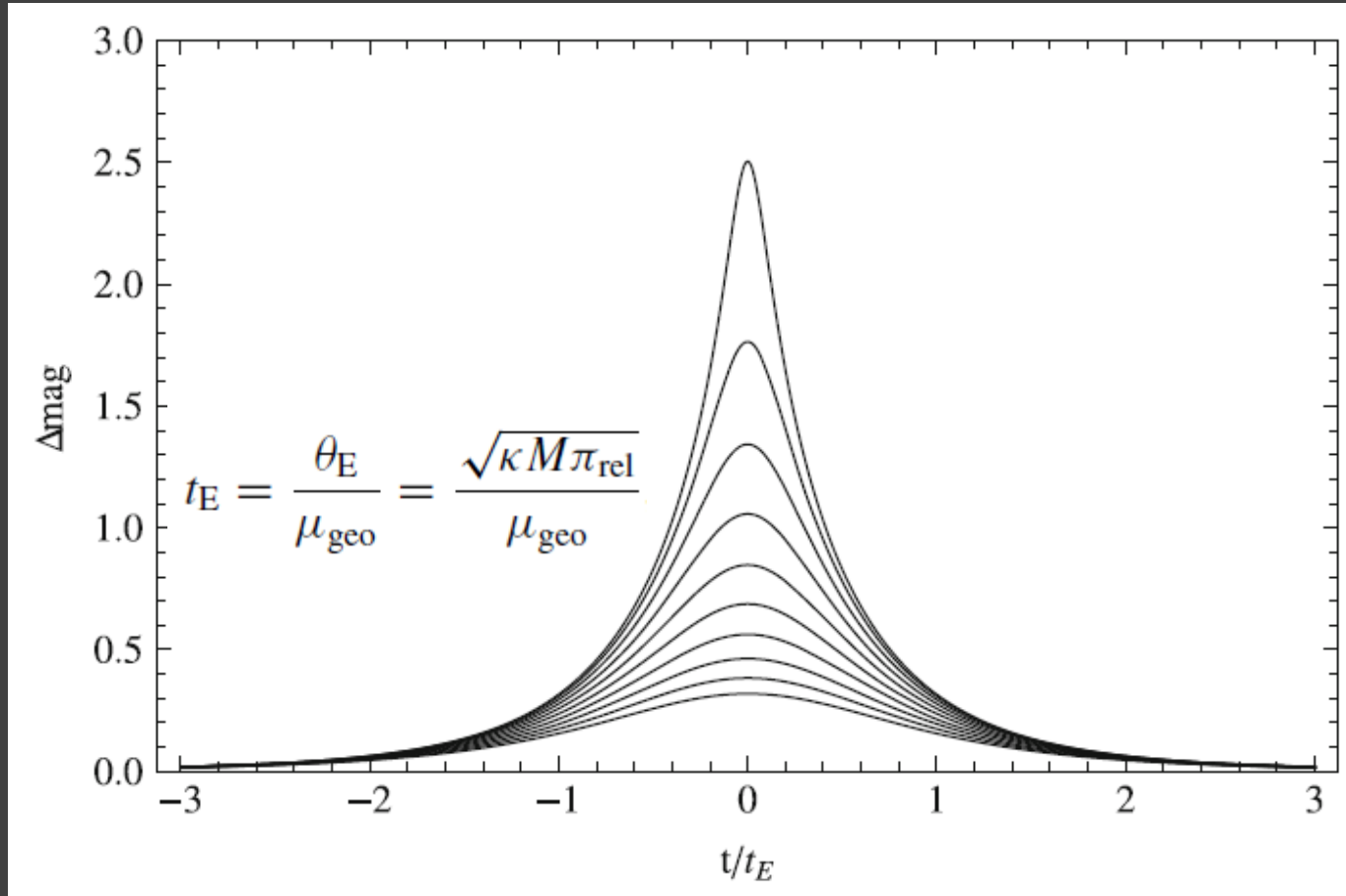
$$\theta_I(\theta_I - \theta_S) = \frac{4GM\pi_{\text{rel}}}{c^2 \text{AU}} \equiv \theta_E^2.$$

$$u_{\pm} = \frac{u \pm \sqrt{u^2 + 4}}{2}; \quad u \equiv \frac{\theta_S}{\theta_E} \quad u_{\pm} \equiv \frac{\theta_{I,\pm}}{\theta_E}.$$

$$A_{\pm} = \pm \frac{u_{\pm}}{u} \frac{\partial u_{\pm}}{\partial u} = \frac{A \pm 1}{2}$$

$$A = \frac{u^2 + 2}{u\sqrt{u^2 + 4}} = (1 - Q^{-2})^{-1/2}; \quad Q \equiv 1 + \frac{u^2}{2},$$

# Light curves for point lenses



$$F(t) = f_s A(\mathbf{u}(t; t_0, u_0, t_E), \rho) + f_b;$$

$$\mathbf{u}(t; t_0, u_0, t_E) = (\tau(t), \beta) = \left( \frac{t - t_0}{t_E}, u_0 \right).$$

# Finite size lense

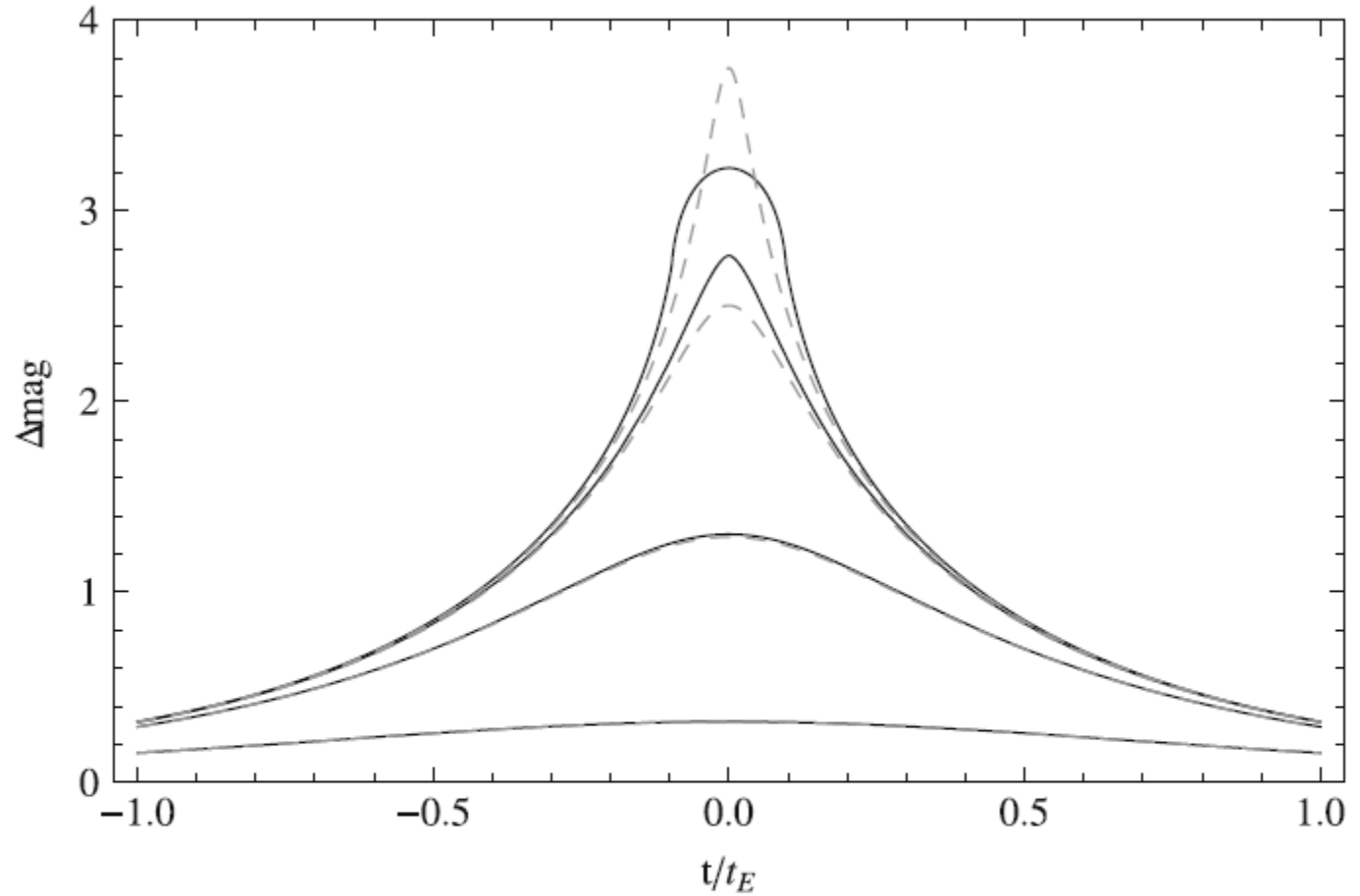
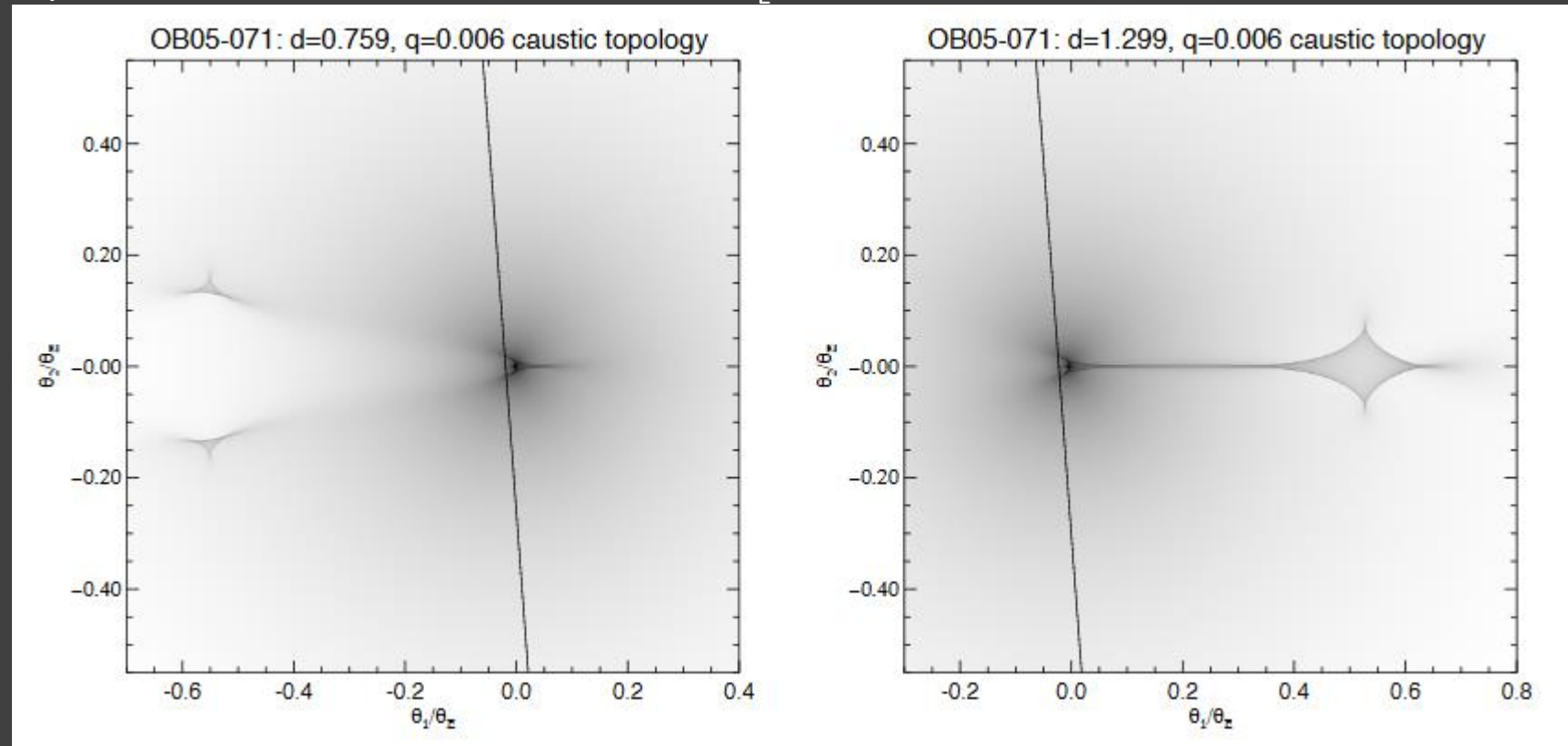


**Fig. 3.4** Magnification as a function of time in microlensing events for an impact parameters  $u_0 = 10^{-n}$  with  $n \in \{-1.5, -1, -0.5, 0\}$ . The angular source size is  $0.1\theta_E$ . Note that when the impact parameter is greater than the source radius, the magnification is higher than the corresponding Paczynski curve (*dashed*). When the impact parameter is smaller than the source radius (source passing right behind the lens), the magnification saturates

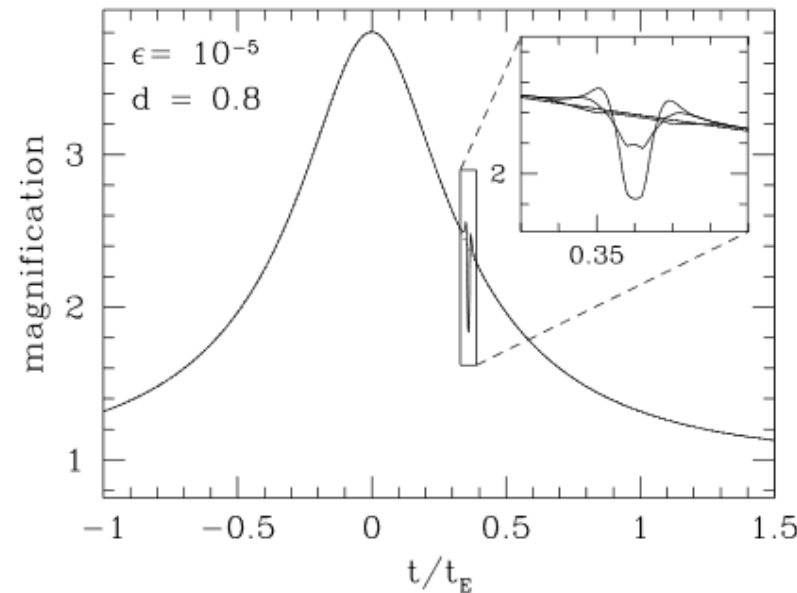
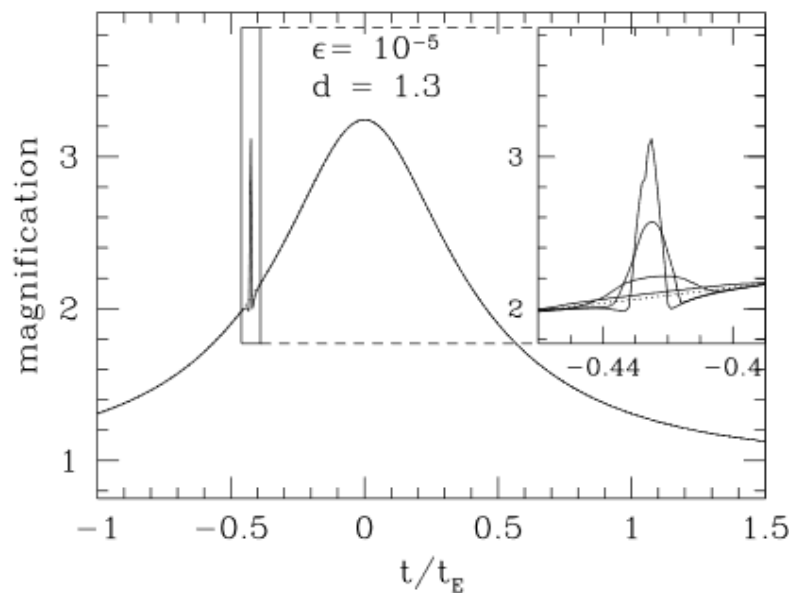
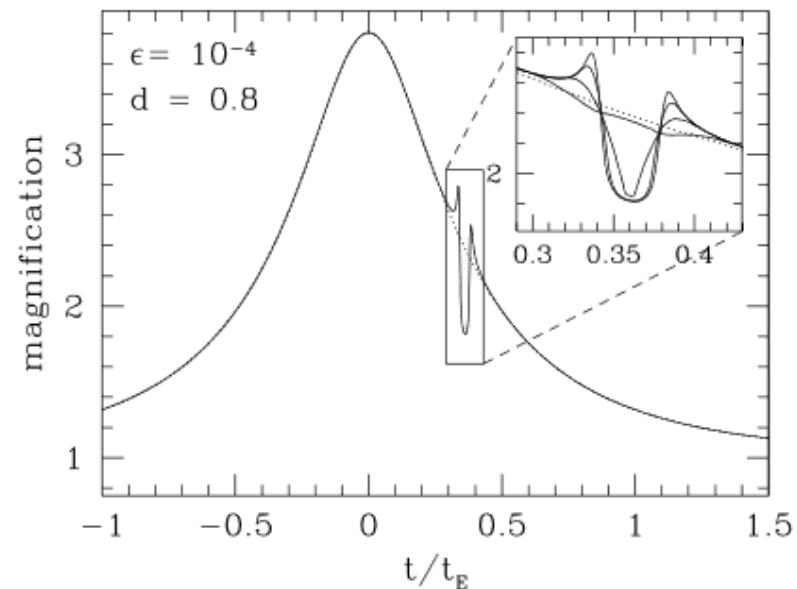
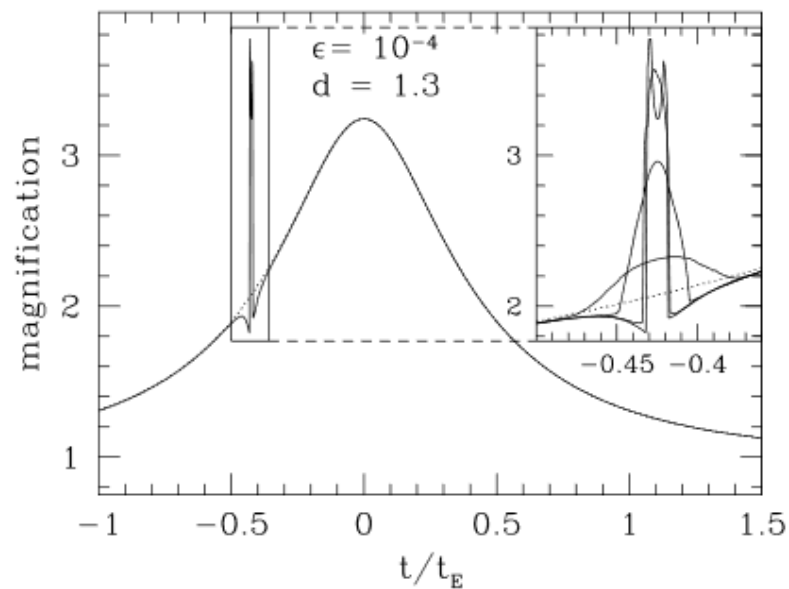
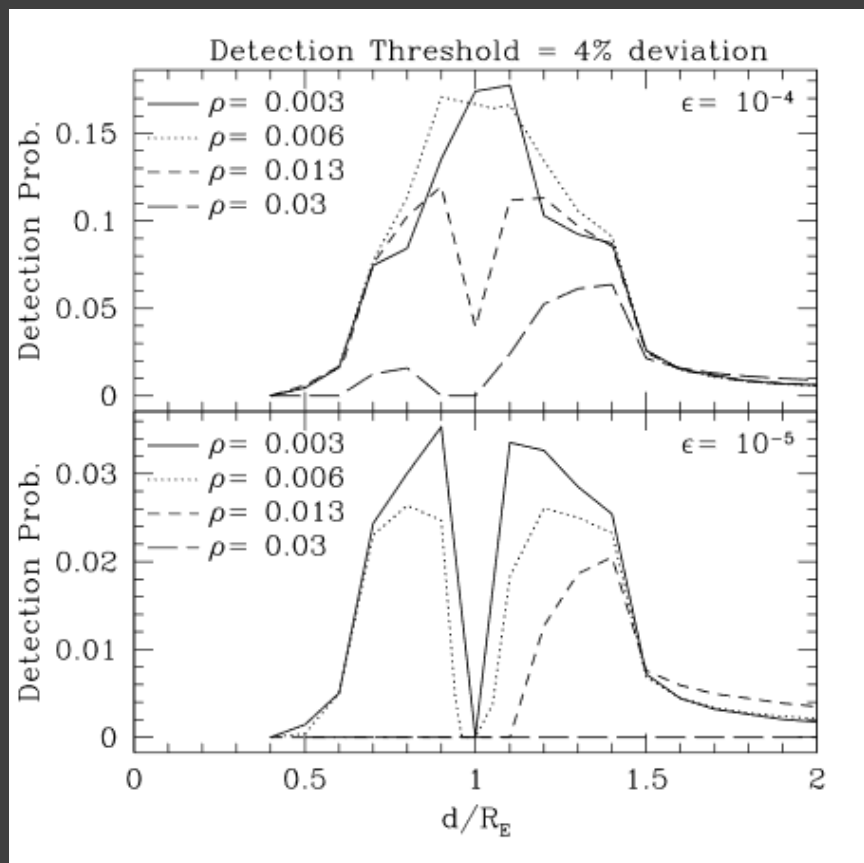
# Binary lense

$s$  – separation of components in units of the Einstein radius  $\theta_E$ .  
 $q$  - mass ratio.

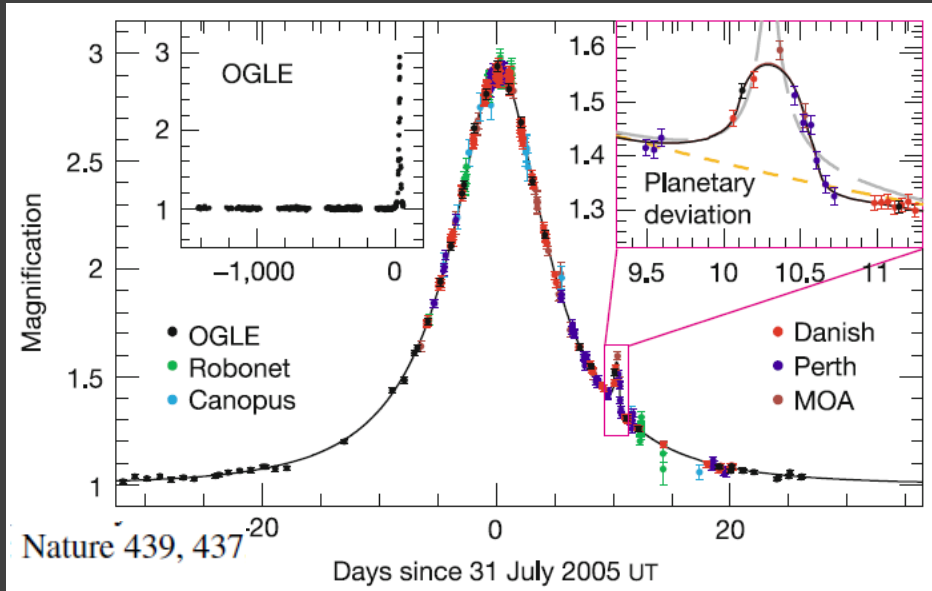
$$r_{\perp} = s\theta_E D_L,$$



# Light curves



# Cold Neptune



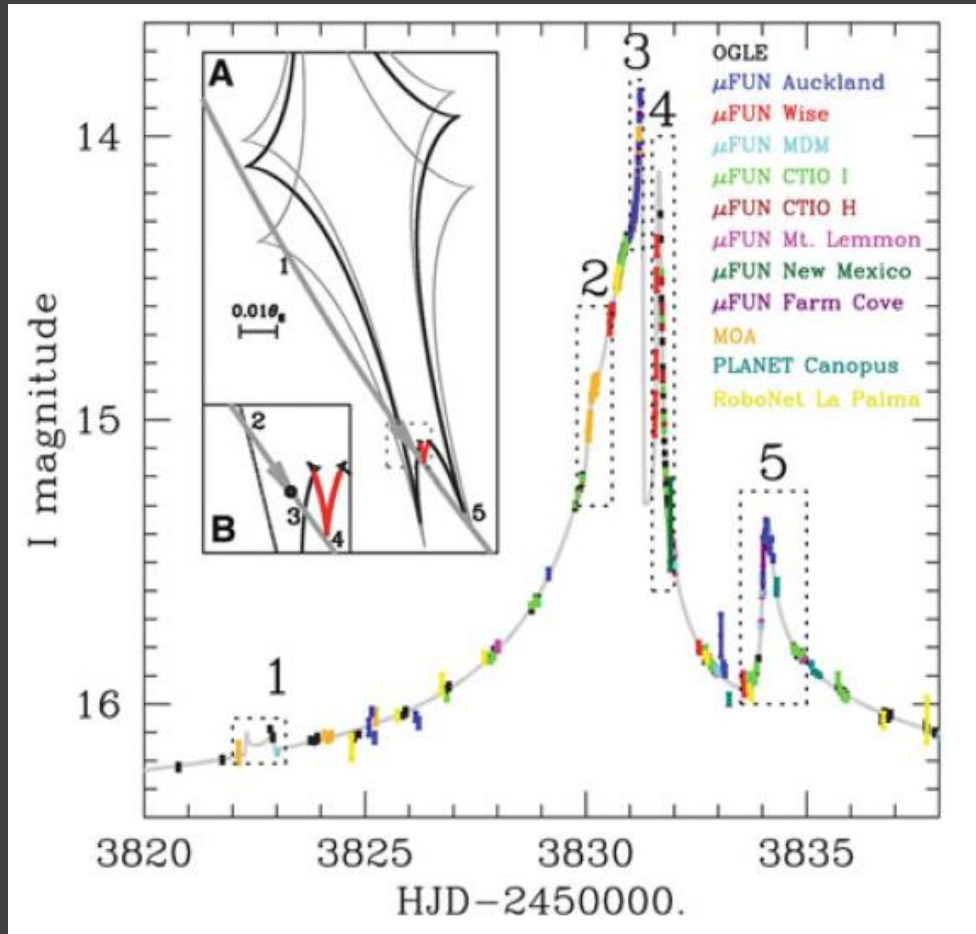
$$A_p = \frac{2}{\rho_p^2} = 2 \left( \frac{\theta_{E,p}}{\theta_*} \right)^2$$

$$\frac{t_p}{t_E} = \frac{\theta_*}{\theta_E}$$

$$q = \frac{m_p}{M} = \frac{\theta_{E,p}^2}{\theta_E^2} = \frac{\theta_{E,p}^2}{\theta_*^2} \frac{\theta_*^2}{\theta_E^2} = \frac{A_p}{2} \frac{t_p^2}{t_E^2} \simeq 1.0 \times 10^{-4}$$

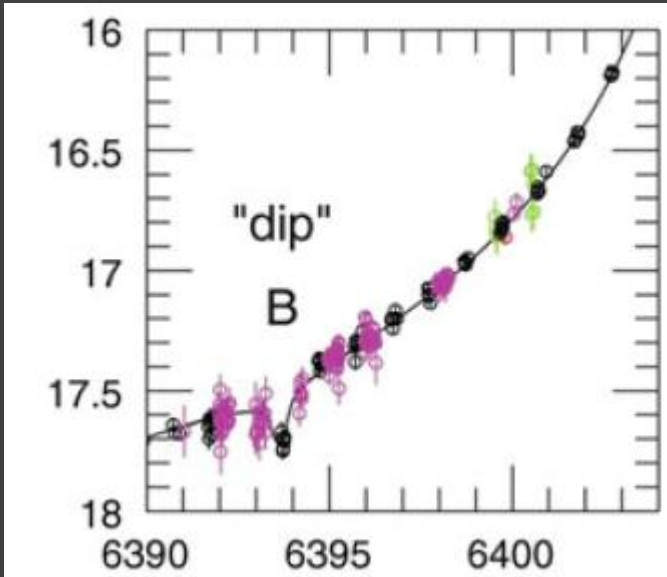
$$r_{\perp} = s \theta_E D_L = 2.2 \text{ AU} \frac{D_L}{8 \text{ kpc}}$$

# Solar system – like system

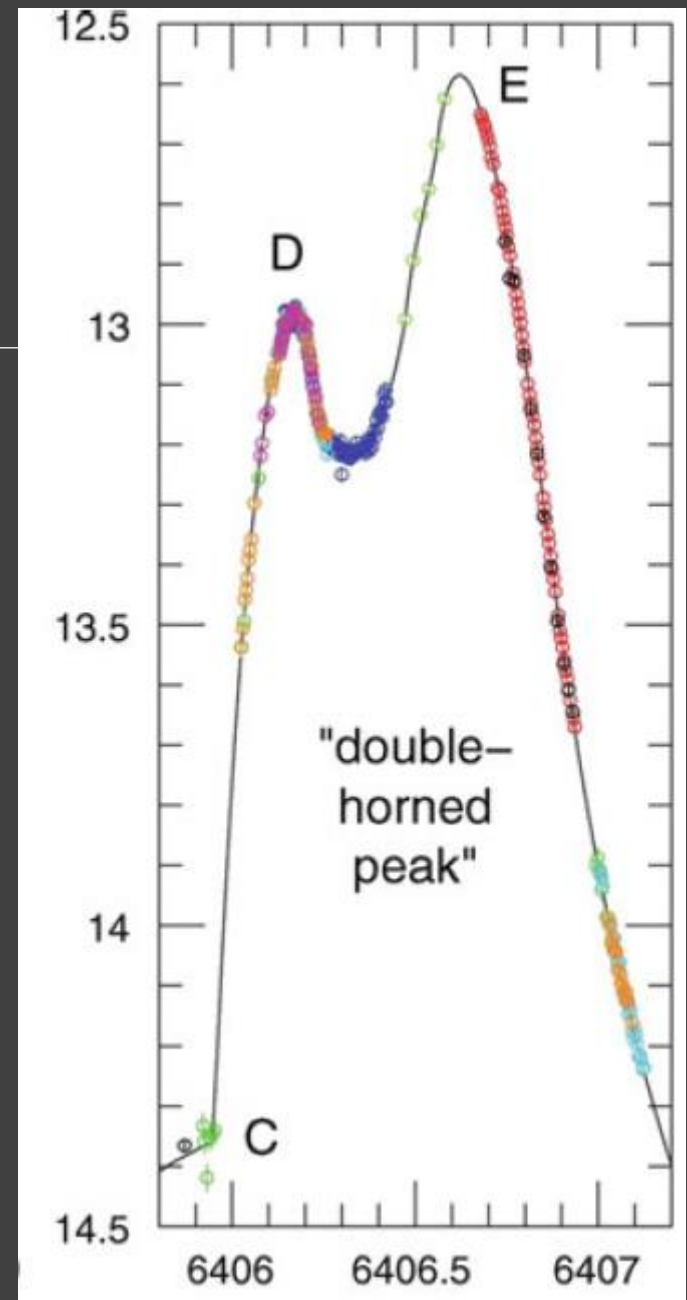


Jupiter and Saturn analogues.  
Distances are slightly smaller  
consistent with smaller mass  
of the host star.

# Dips due to planets

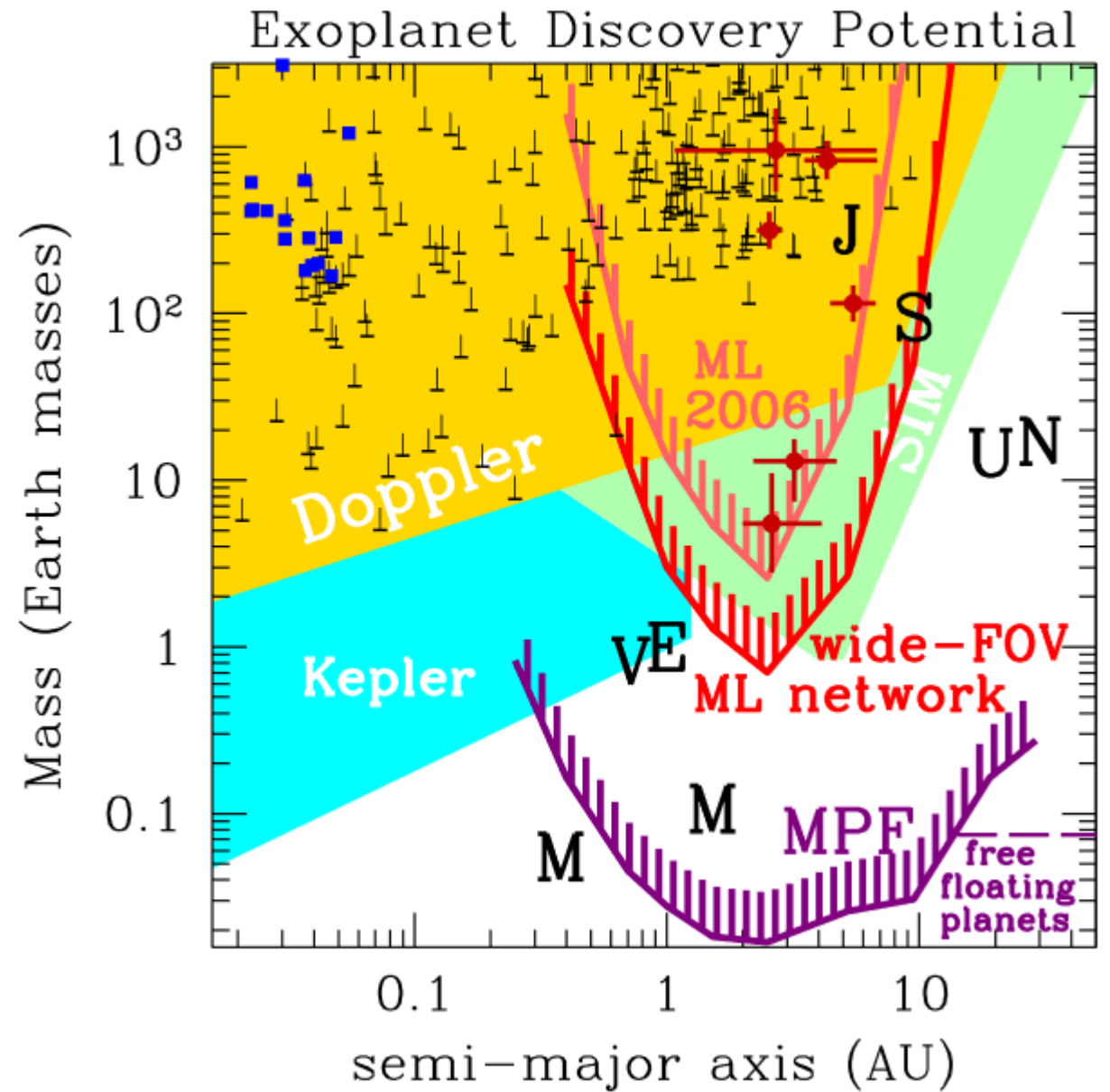
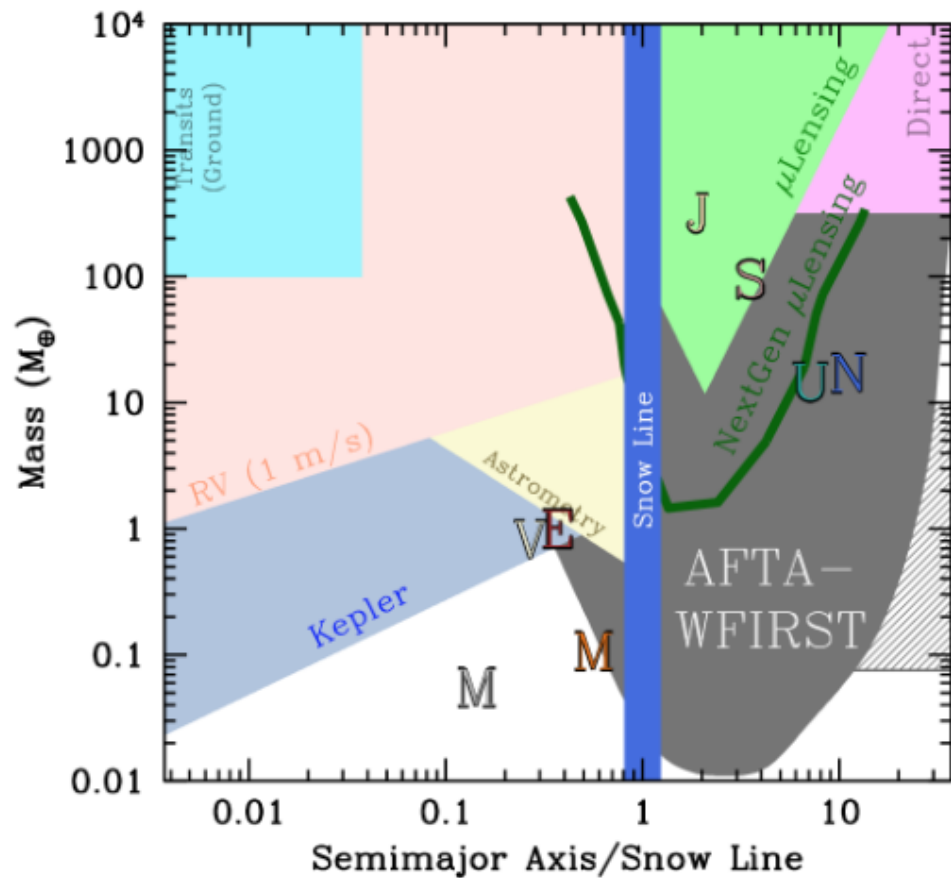


A terrestrial-mass planet in a binary. The planet orbits a red dwarf (1 AU), which orbits another star (15 AU)

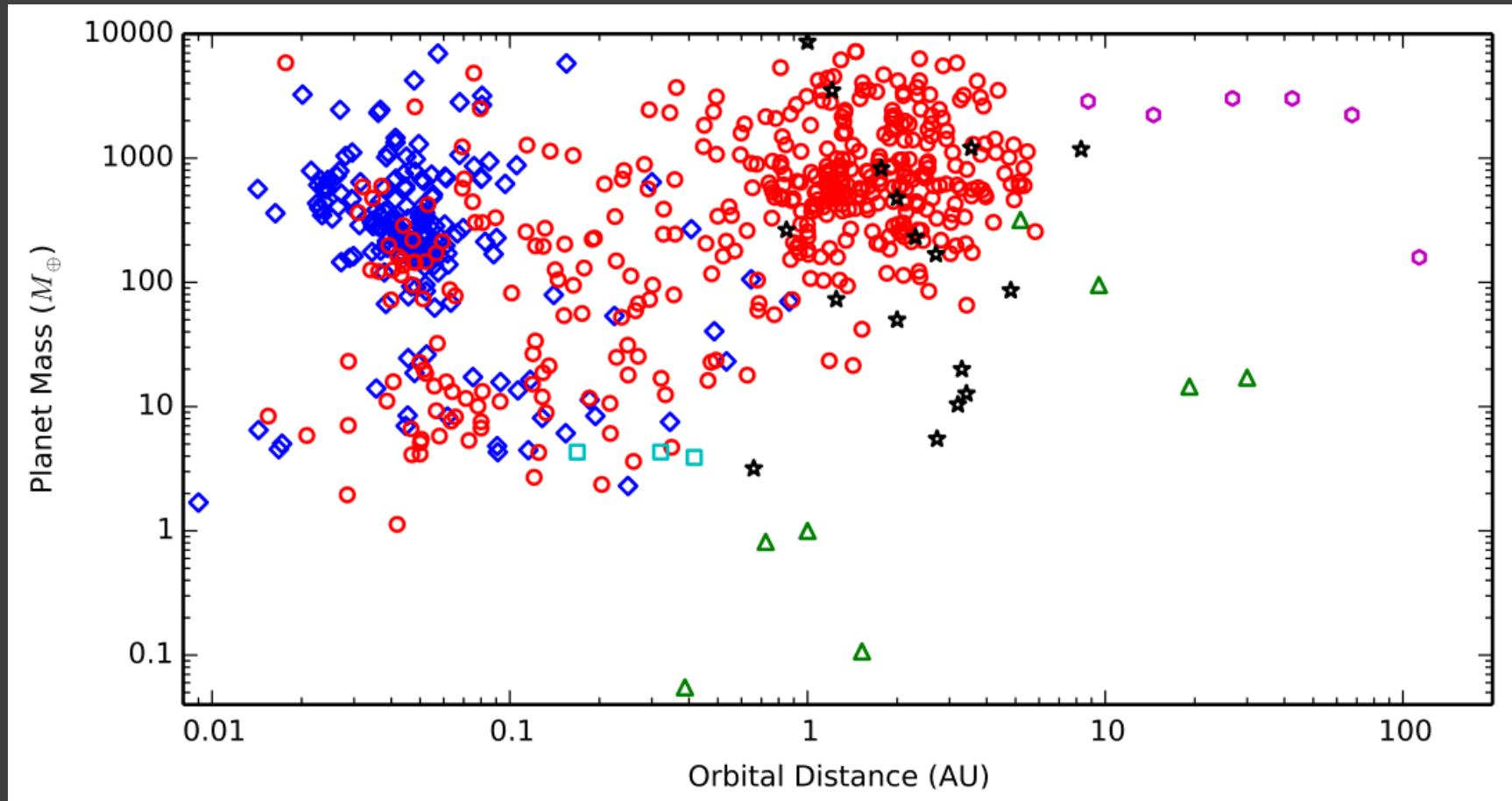




# Comparison of three methods



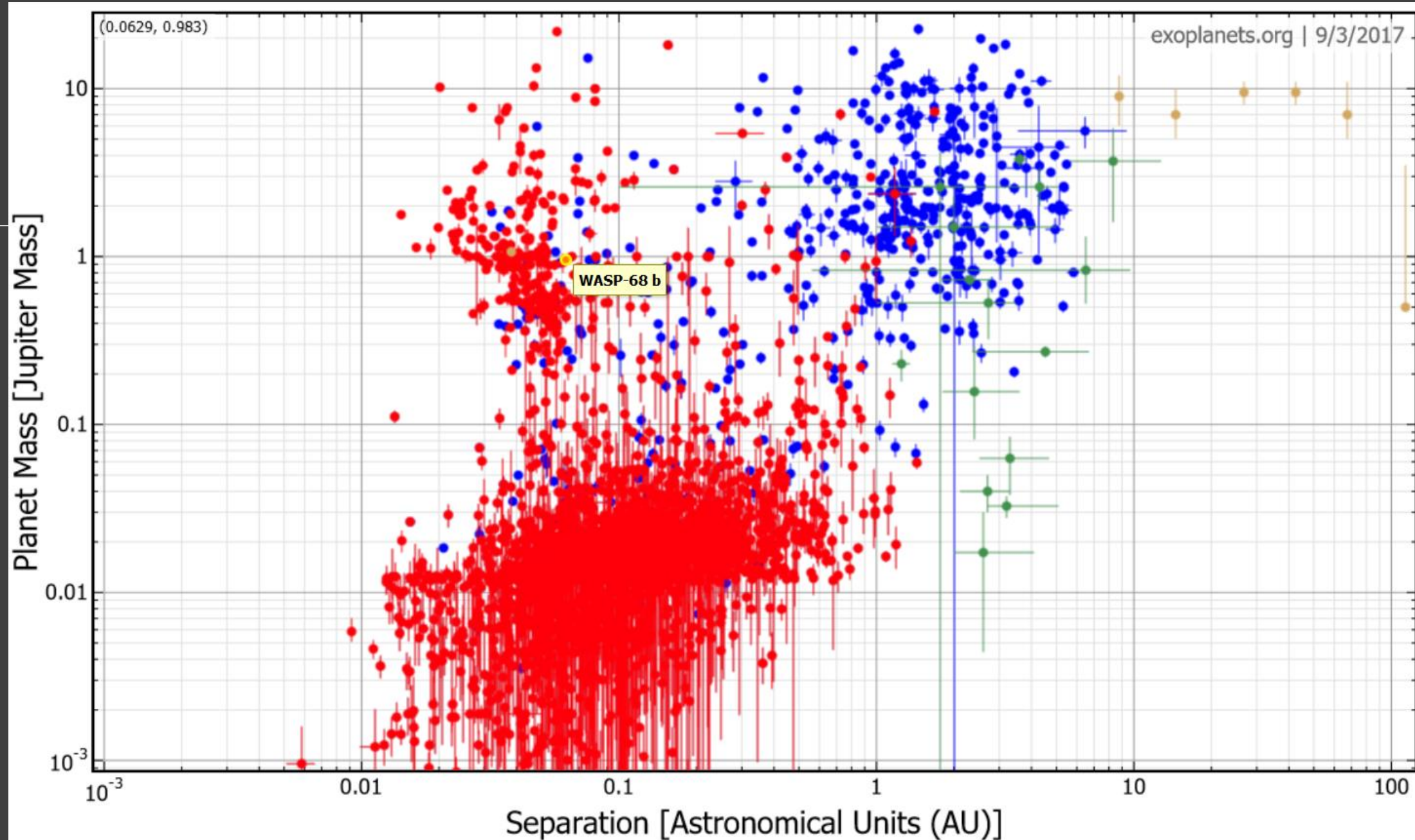
# Discoveries by different methods



RV = red circles,  
transit = blue diamonds,  
imaging = magenta hex.,  
gravlens = black stars,  
psr time = cyan squares.

Planets in the Solar  
System are green  
triangles.

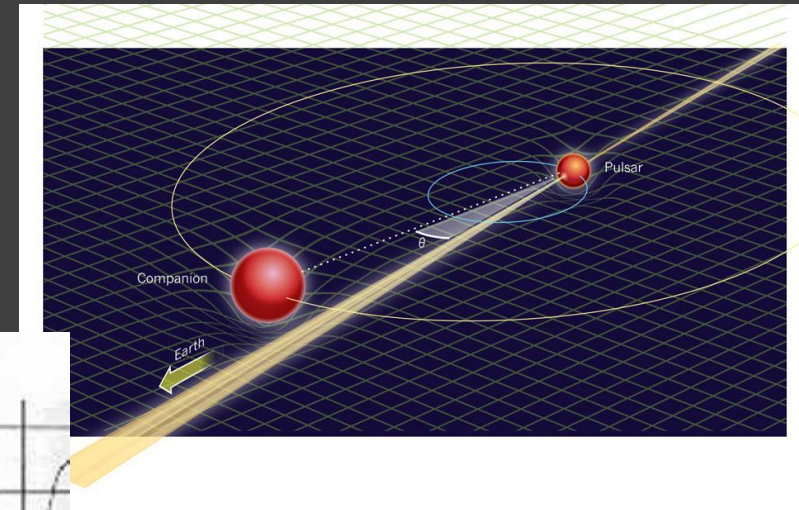
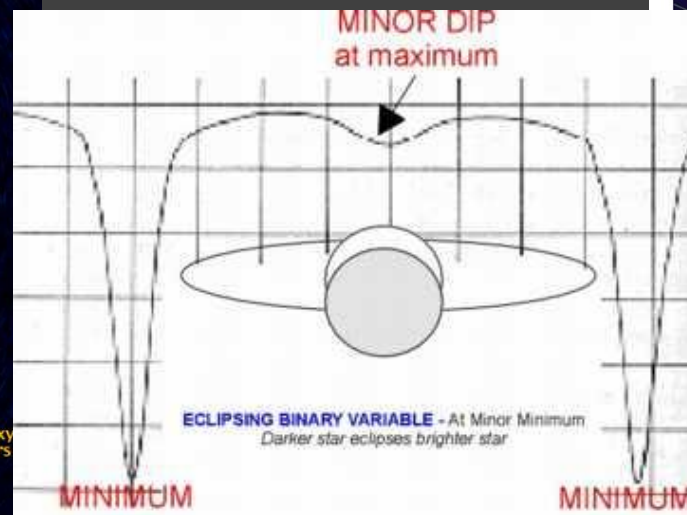
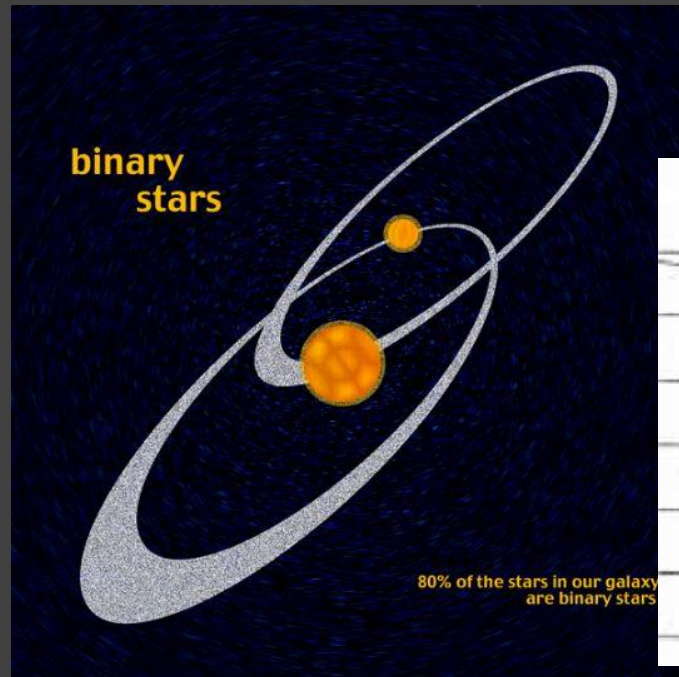
Blue- RV  
Red – Trans.  
Green – lense  
Orange –  
imaging





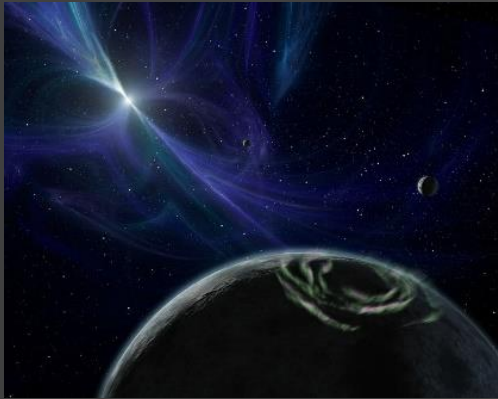
# Timing

Observations of a periodic process  
(radio pulsar, binary system, pulsating star)  
allows to identify a perturber



# Planets around a radio pulsar

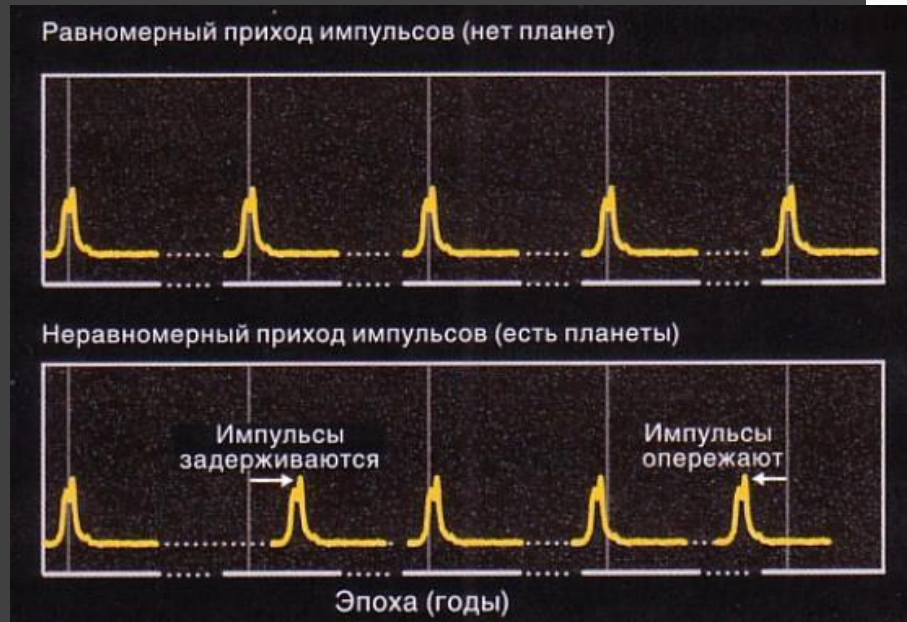
Wolszczan, Frail 1992



PSR B1257+12  
Millisecond pulsar

Three light planets

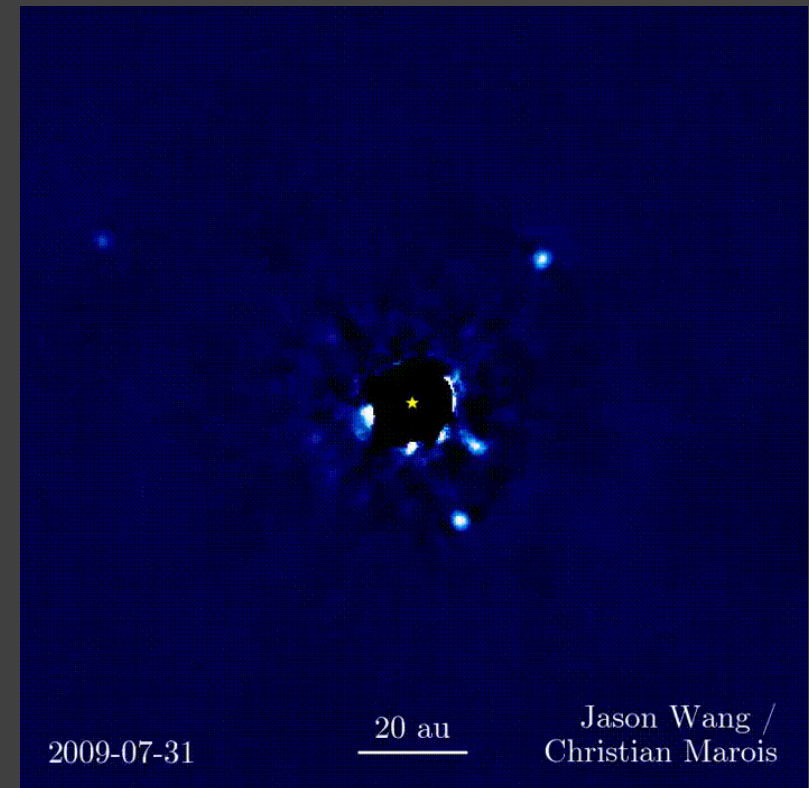
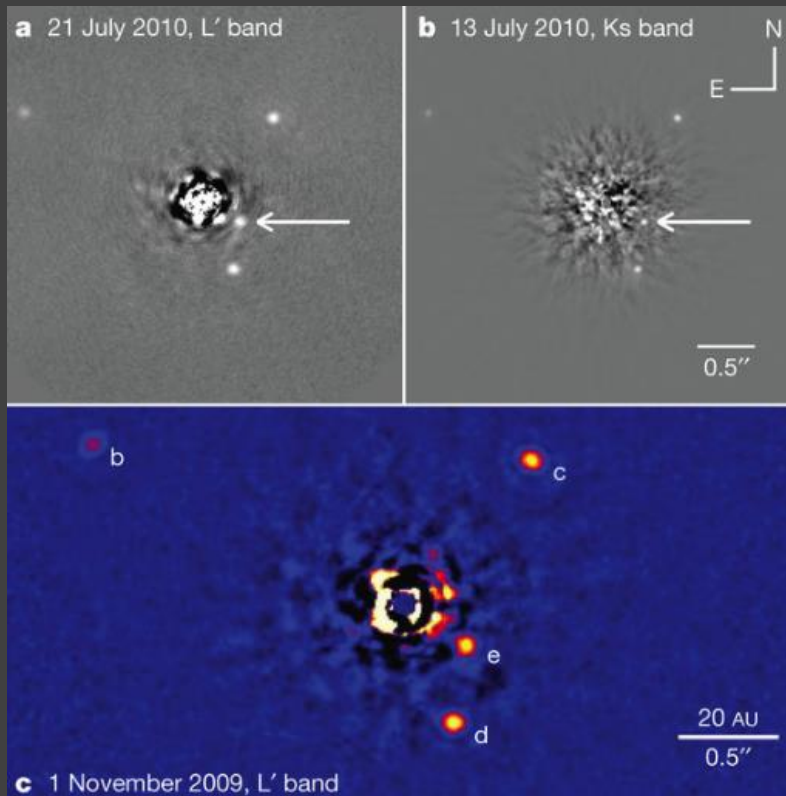
Companion (in order from star)	Mass	Semimajor axis (AU)	Orbital period (days)
A (b)	$0.020 \pm 0.002 M_{\oplus}$	0.19	$25.262 \pm 0.003$
B (c)	$4.3 \pm 0.2 M_{\oplus}$	0.36	$66.5419 \pm 0.0001$
C (d)	$3.9 \pm 0.2 M_{\oplus}$	0.46	$98.2114 \pm 0.0002$



# Direct imaging

Now it is possible to see self-luminous planets ( $10^{-5}$  in flux) at  $>\sim 1$  arcsec.

For comparison: Solar system analogue at 10 pc gives for Jupiter  $10^{-9}$  in flux and 0.5 arcsec.



# Telescope properties

Instrument	Telescope	Wavelength ( $\mu\text{m}$ )	Ang. resol. (mas)	Coronagraph
ACS	HST	0.2–1.1	20–100	Lyot
STIS	HST	0.2–0.8	20–60	Lyot
NAOS–CONICA	VLT	1.1–3.5	30–90	Lyot/FQPM
VISIR	VLT	8.5–20	200–500	—
SINFONI–SPIFFI	VLT	1.1–2.45	28–62	—
SPHERE	VLT	0.95–2.32	24–62	Lyot/APLC/FQPM
PUEO	CFHT	0.75–2.5	4–140	Lyot
CIAO	SUBARU	1.1–2.5	30–70	Lyot
OSIRIS	Keck I	1.0–2.4	20–100	—
AO–NIRC2	Keck II	0.9–5.0	20–100	Lyot
ALTAIR–NIRI	Gemini N.	1.1–2.5	30–70	Lyot
GPI	Gemini S.	0.9–2.4	24–62	Lyot/APLC
PALM-3000 PHARO	Hale 200''	1.1–2.5	60–140	Lyot/FQPM
PALM-3000 Project1640	Hale 200''	1.06–1.76	43–71	APLC
AO–IRCAL	Shane 120''	1.1–2.5	100–150	—

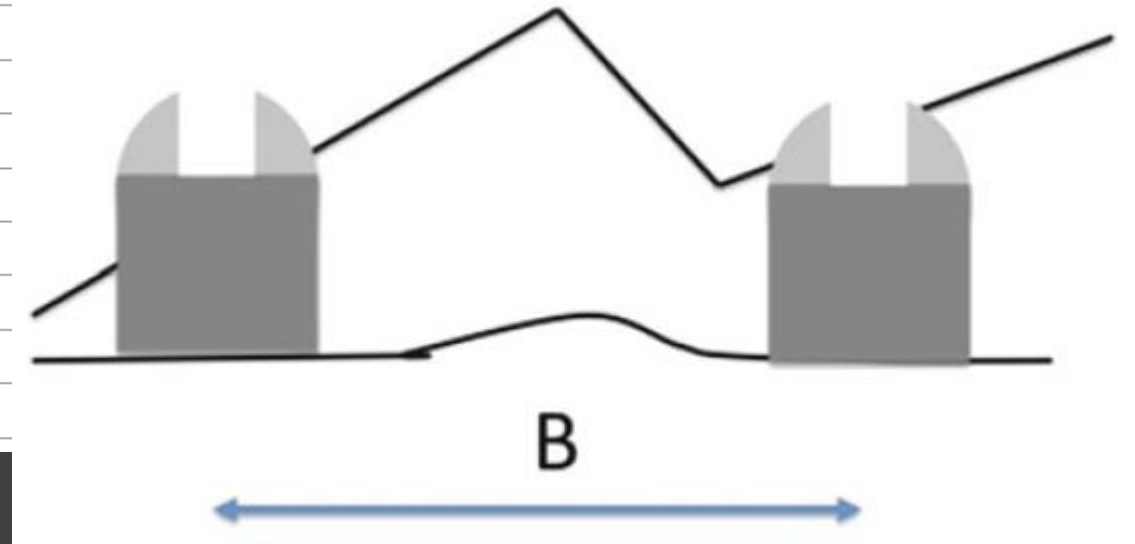
$$\Theta = (a/d)(1+e) = 1 \text{ arcsec } (a/\text{AU})(d/\text{pc})^{-1} (1+e)$$



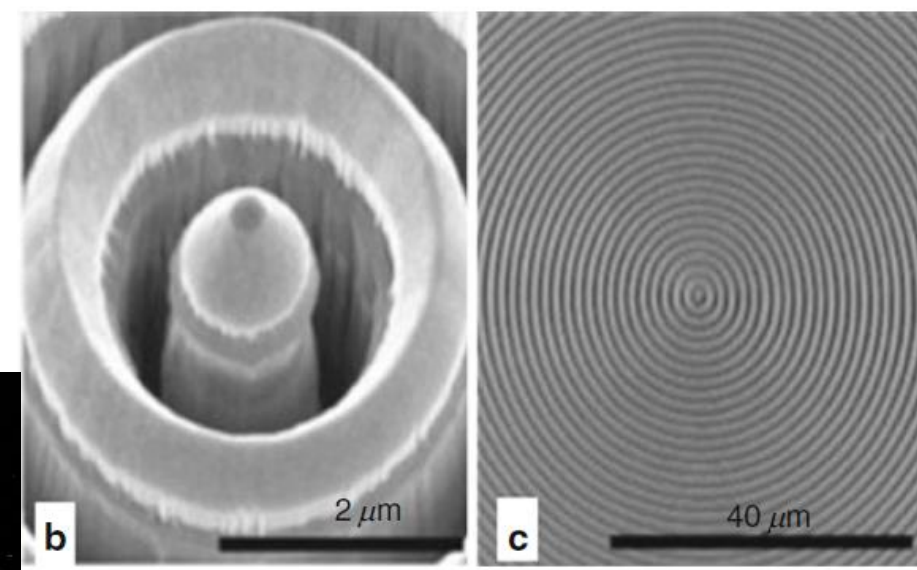
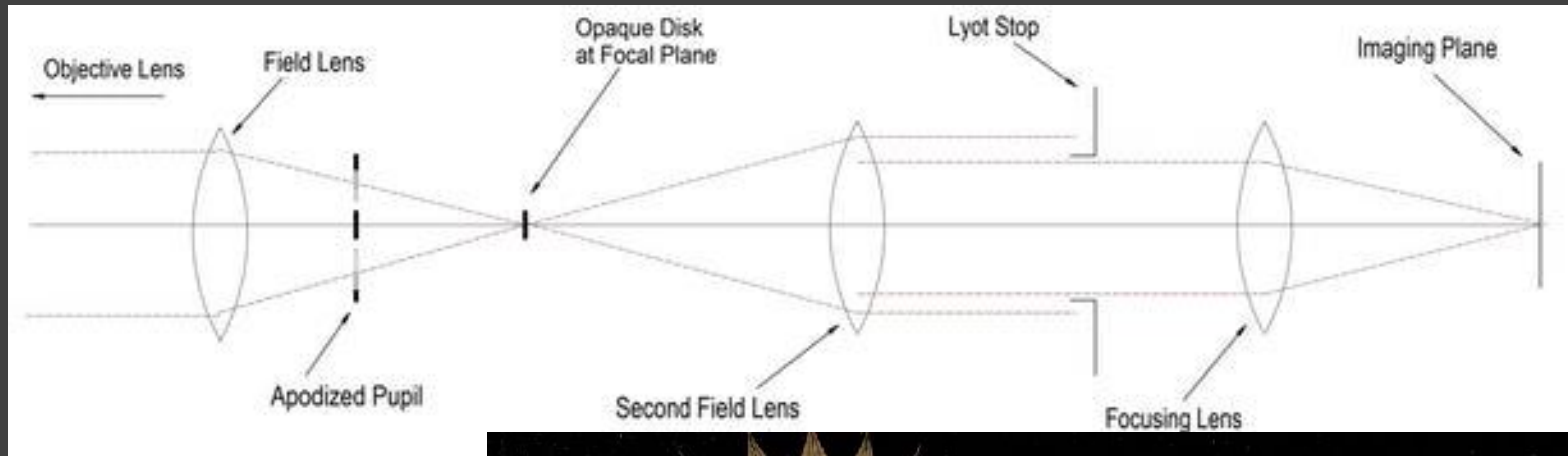
# Ground optical interferometers

Instrument	Interf.	Baseline (m)	Bands	Ang. res. (mas)	Spec. res.	Aperture
AMBER	VLTI	16–200	J,H,K	0.6–14	35–15,000	3
MIDI	VLTI	16–200	N	4–80	20–220	2
PIONIER	VLTI	16–200	H,K	1.5–45	15	4
V2	Keck I	85	H,K,L	2–5	25–1800	2
Nuller	Keck I	85	N	10–16	40	2
Mask	Keck	1–10	J to L	13–400	None	2
Classic	CHARA	34–330	H,K	0.5–7	None	2
FLUOR	CHARA	34–330	K	0.7–7	None	2
MIRC	CHARA	34–330	J,H	0.4–5	40–400	4
BLINC	MMT	4	N	250	None	2
LMIRCAM	LBTI	14–23	L,M	27–72	None	2
NOMIC	LBTI	14–23	N	72–200	None	2

Better resolution,  
but smaller aperture

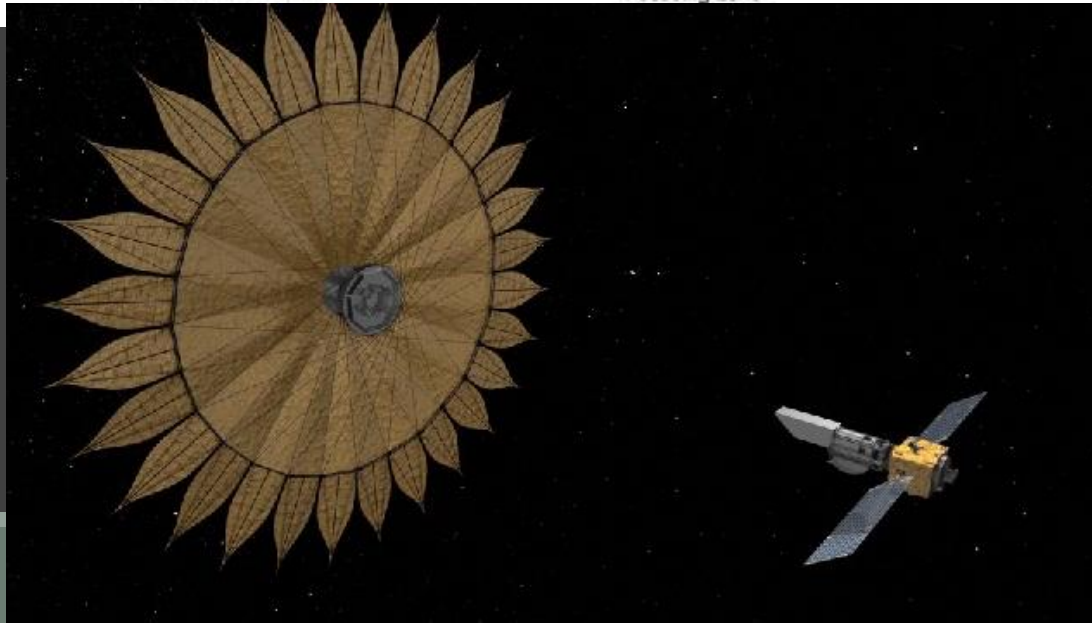


# Coronagraphs

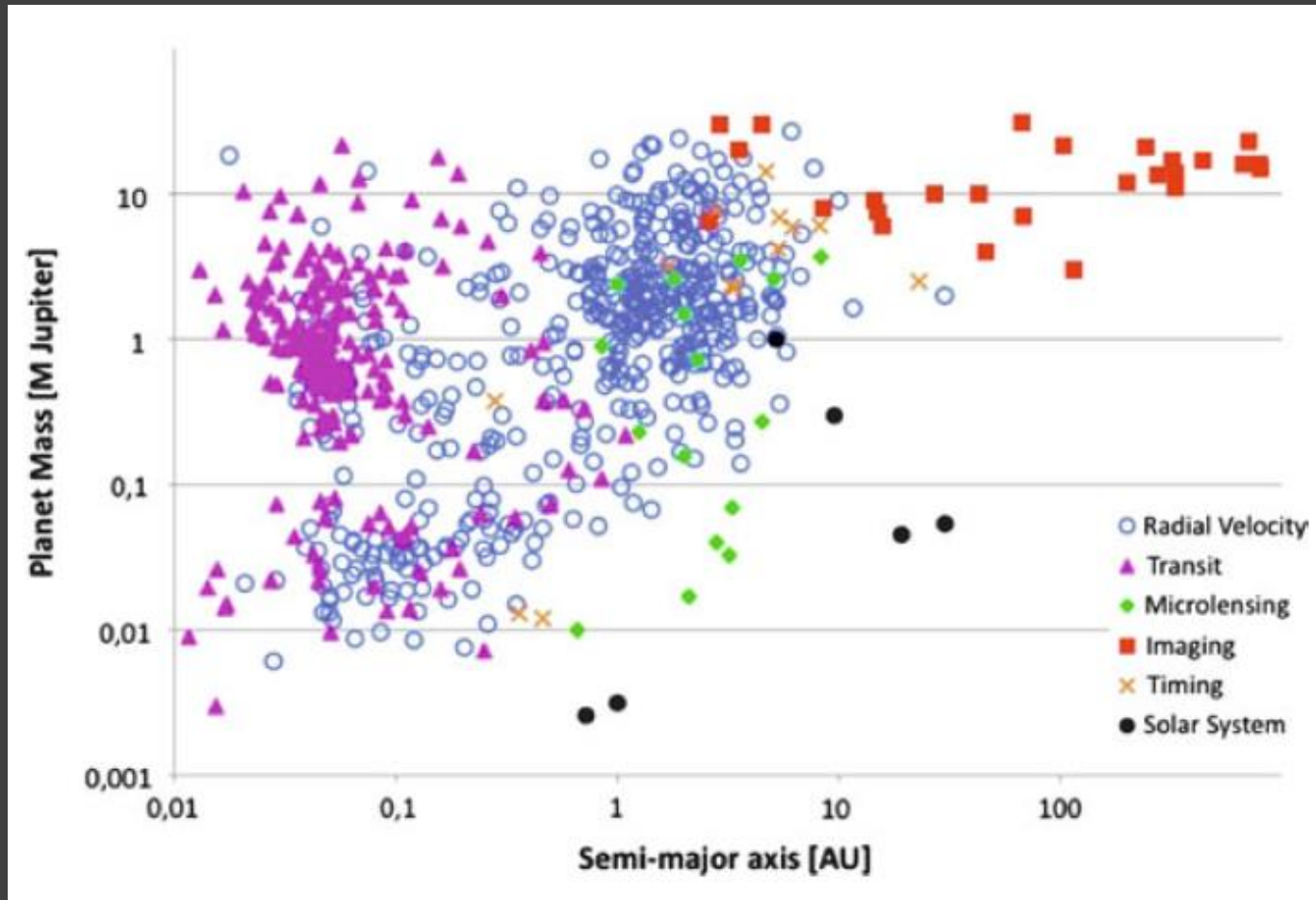


Riccardo Claudi (in Bozza et al. 2016)

To obtain planet images different kinds of coronagraphs are used.



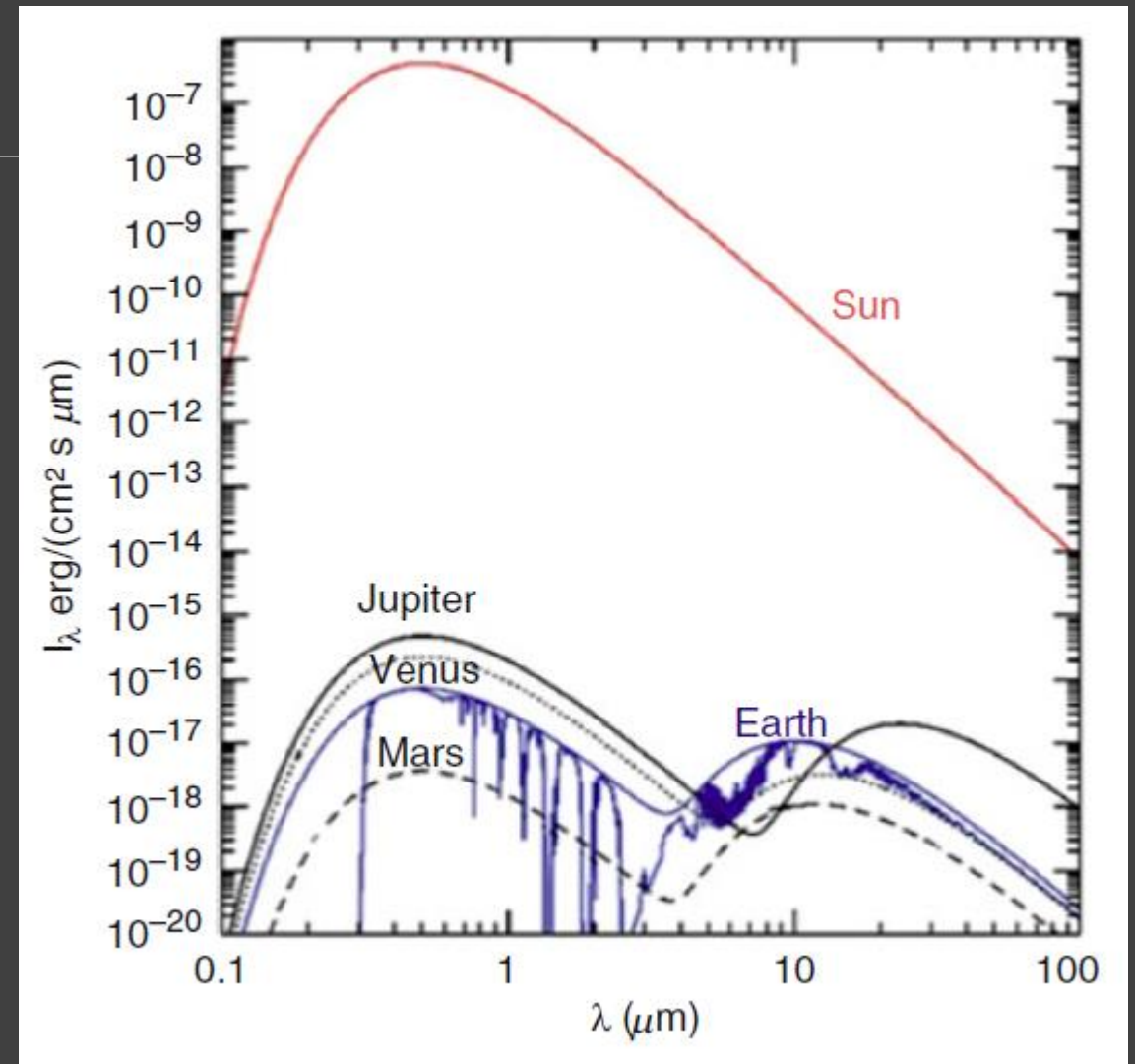
# Imaging vs. other methods



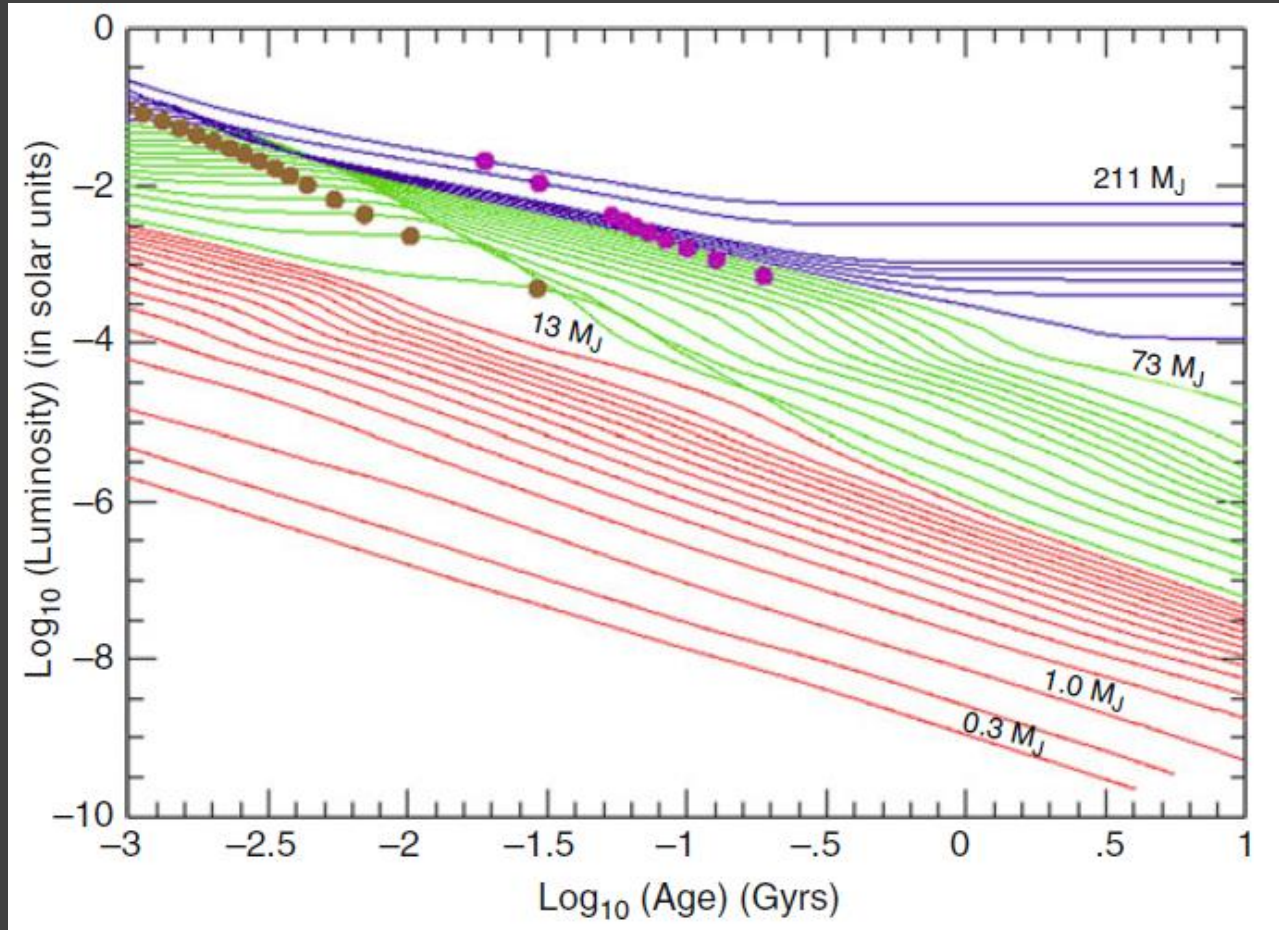
# Solar system

Notice, how much better planets are visible in IR.  
Especially Jupiter at 20-30 micrometers.

$$F_{p, \text{vis}} = A(\lambda, t) \phi(t) \frac{R_p^2}{4a^2} B(\lambda, T_{\text{eff}}) R_{\star}^2,$$



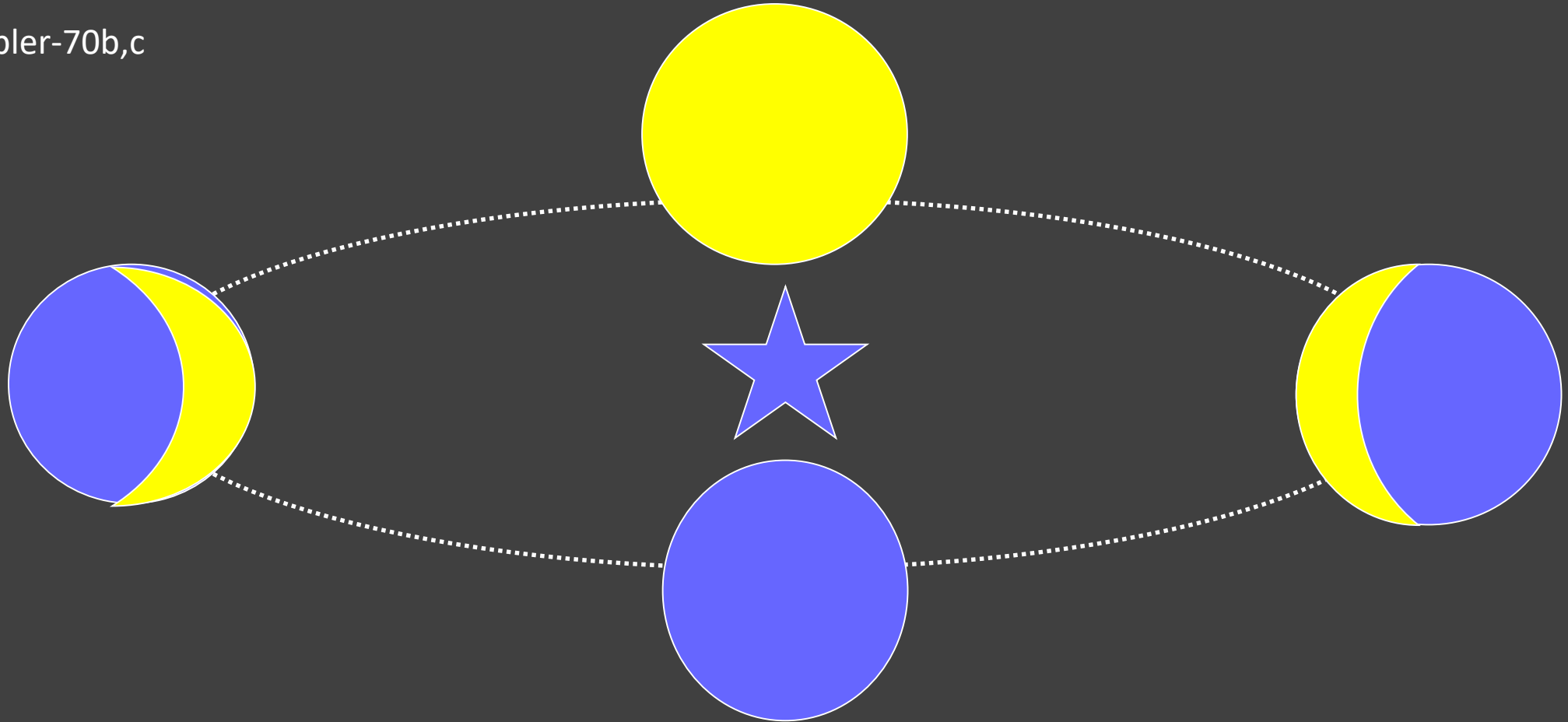
# Young planets are hotter



# Planet light identification

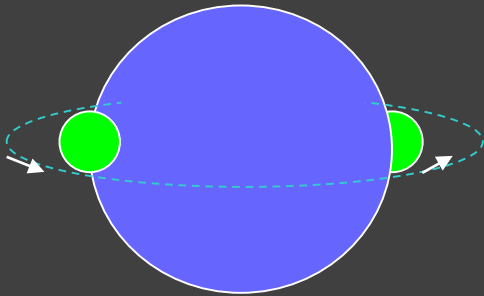
---

Kepler-70b,c





# IR light



55 Cnc e

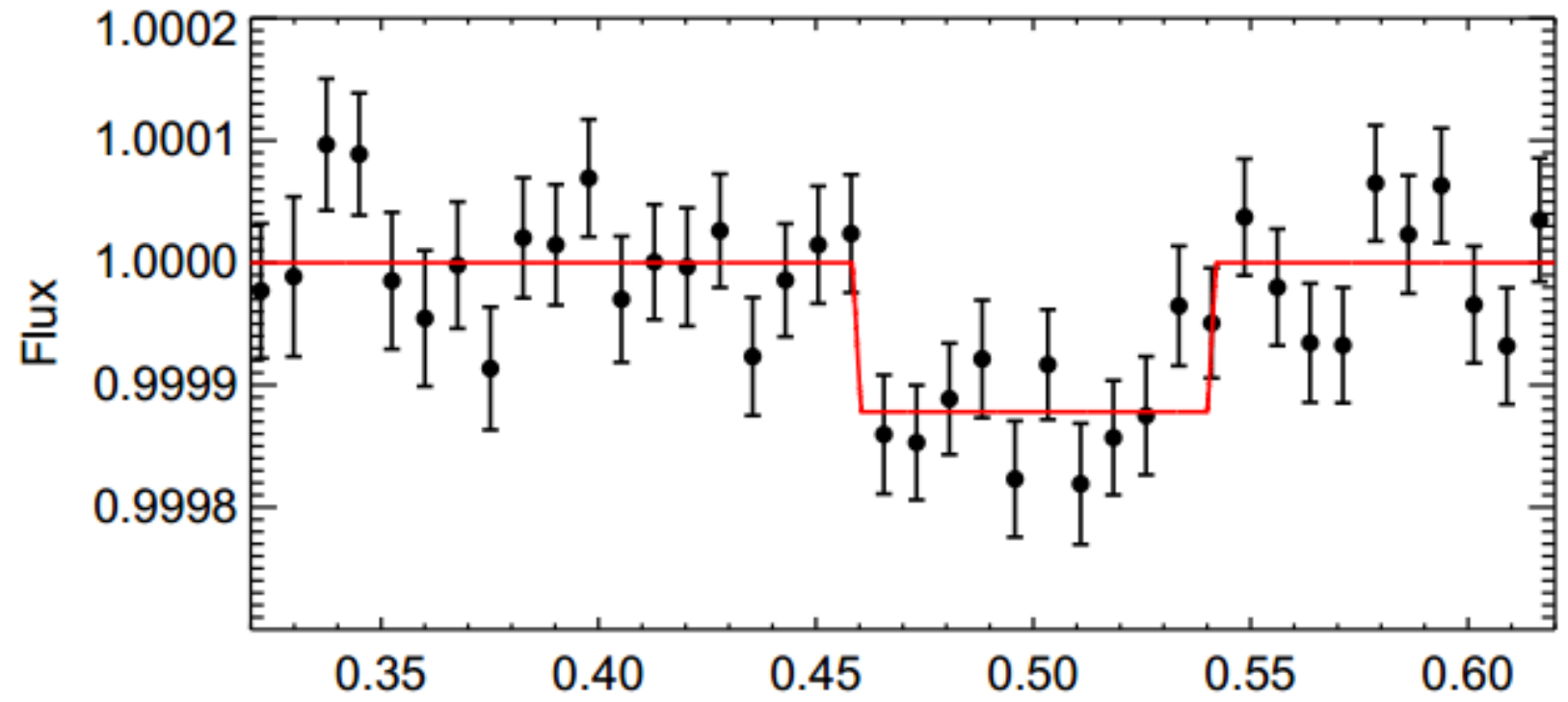
Mass: 7-8 Earth mass

Semi-major axis: 0.016 AU

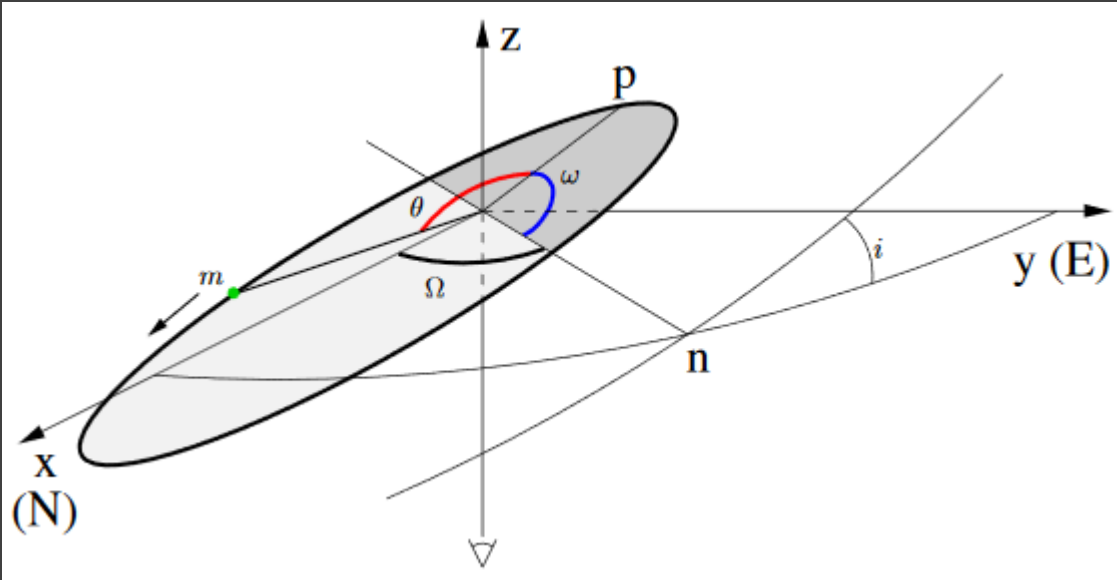
Orbital period: 0.74 days

Temperature 2000-2600K

Occultation light curve



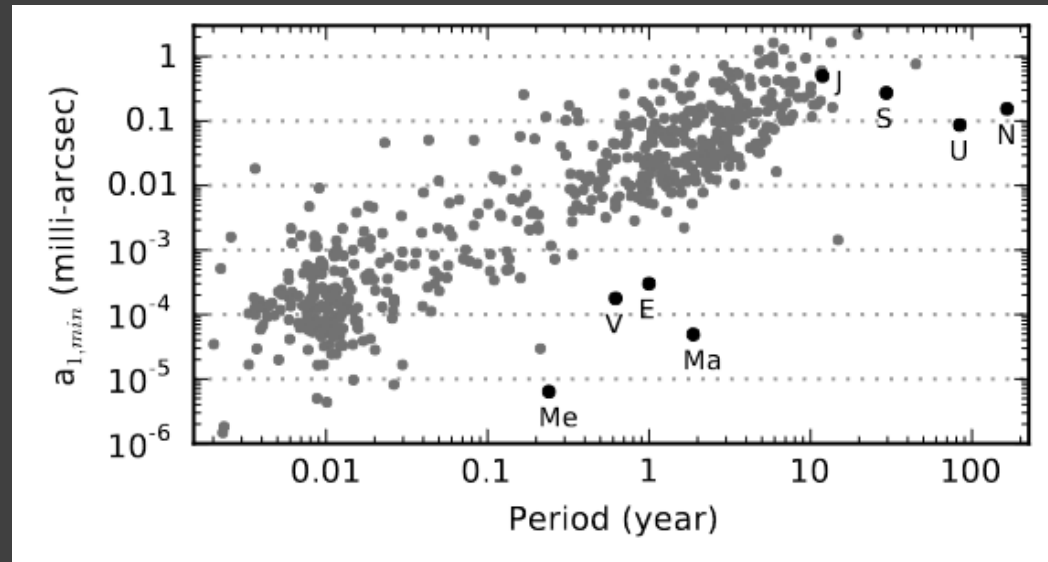
# Astrometric detection



$$4\pi^2 \frac{\bar{a}_1^3}{P^2} = G \frac{M_P^3}{(M_* + M_P)^2},$$

It is easier to detect massive long period planets on eccentric orbits.

Astrometry allows to determine  $M_{\text{planet}}^3 / (M_{\text{star}} + M_{\text{planet}})^2$



Data on 570 stars with planets are shown.  
Solar system data is scaled for a star at 10 pc.

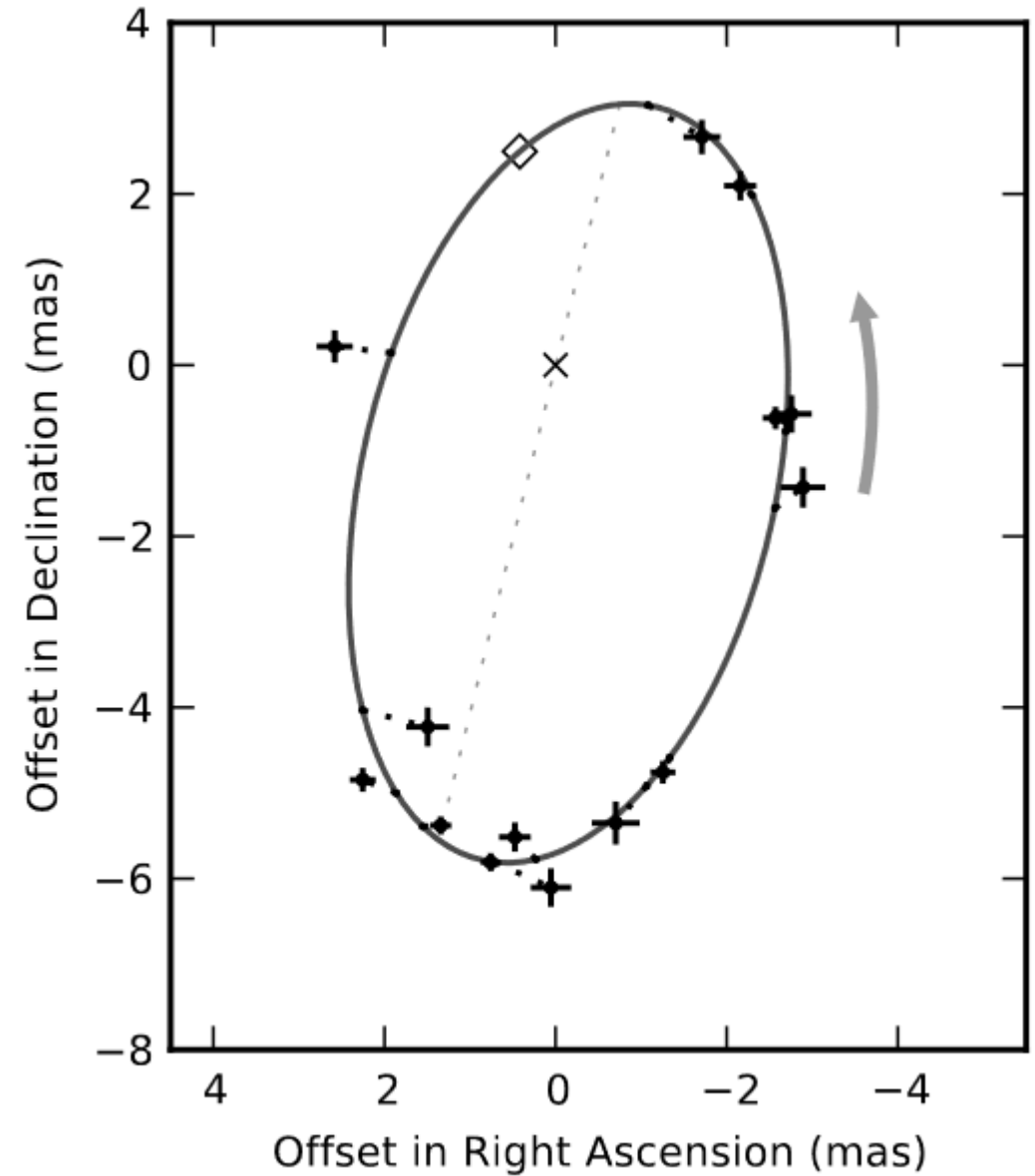


# The only candidate

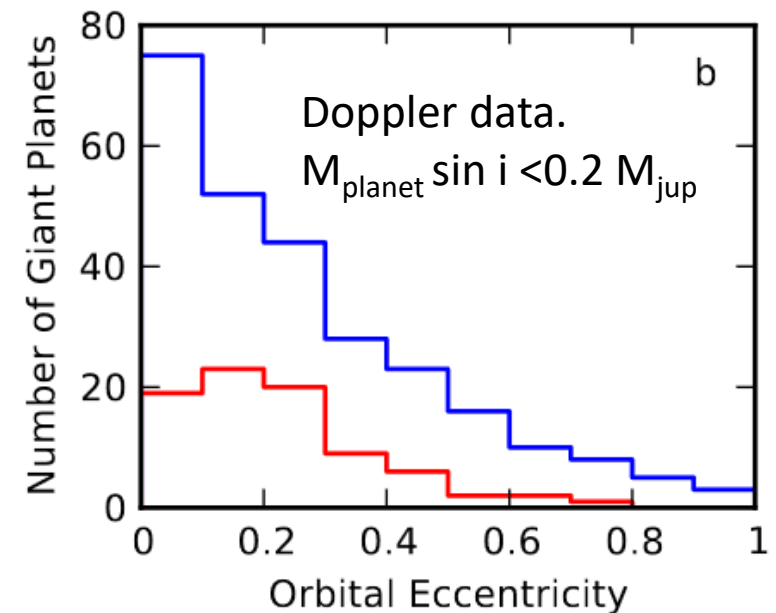
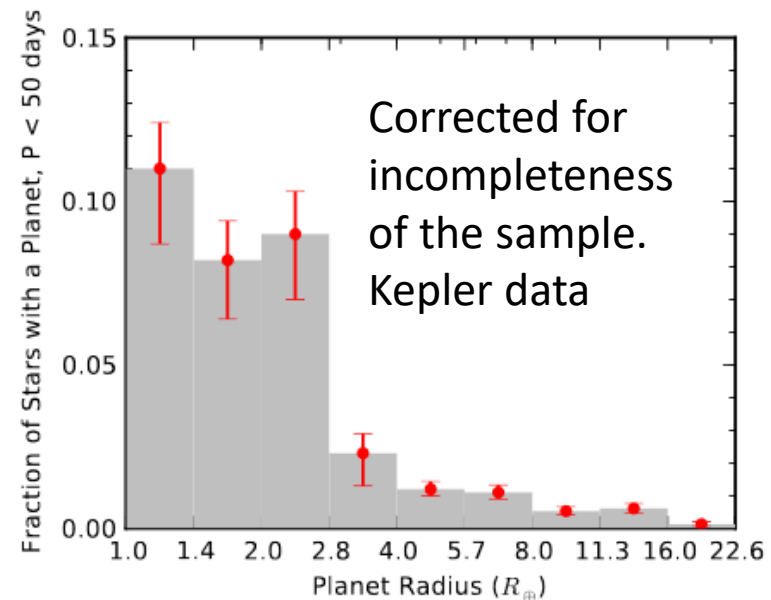
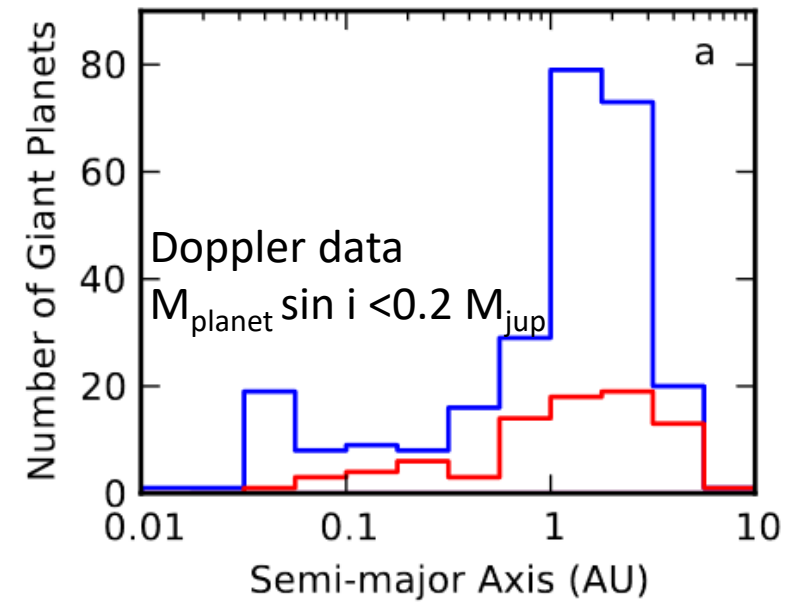
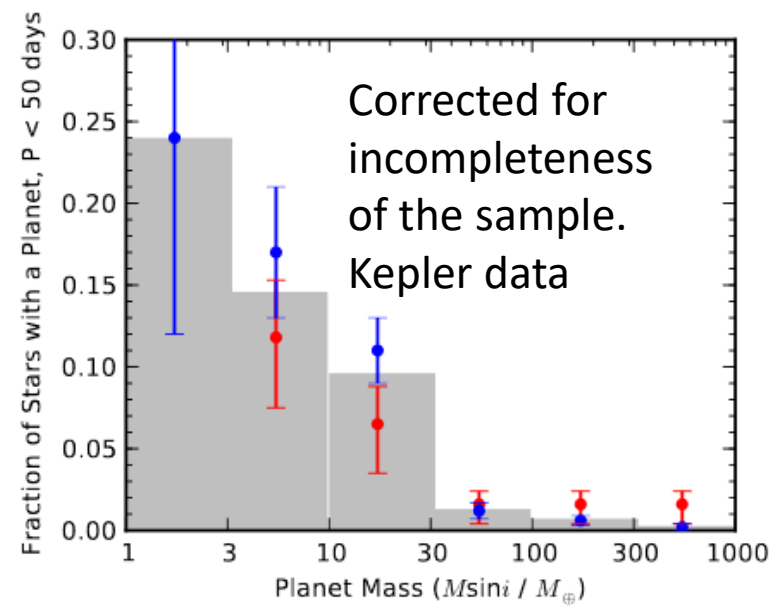
Came out to be a brown dwarf with  $28 M_{\text{Jup}}$ .

Now waiting for Gaia data.

Fig. 15.— The barycentric orbit of the L1.5 dwarf DENIS-P J082303.1-491201 caused by a 28 Jupiter mass companion in a 246 day orbit discovered through ground-based astrometry with an optical camera on an 8 m telescope ([Sahlmann et al., 2013a](#)).



# Planetary statistics



# Literature

---

arxiv:1505.06869 Exoplanet Detection Techniques

arxiv:1504.04017 The Next Great Exoplanet Hunt

arxiv:1410.4199 The Occurrence and Architecture of Exoplanetary Systems

arXiv:1708.00896 Timing by Stellar Pulsations as an Exoplanet Discovery Method

arxiv:1706.09849 Transit Timing and Duration Variations for the Discovery and Characterization of Exoplanets

arxiv:1705.05791 Exoplanet Biosignatures: A Review of Remotely Detectable Signs of Life

arxiv:1704.07832 Mapping Exoplanets

arxiv:1701.05205 Characterizing Exoplanets for Habitability

arxiv:1411.1173 Astrometric exoplanet detection with Gaia

arxiv:1001.2010 Transits and Occultations

arxiv:0904.0965 Astrometric detection of earthlike planets

arXiv:0904.1100 Exoplanet search with astrometry

arxiv:0902.1761 Detection of extrasolar planets by gravitational microlensing

